University of Stavanger

FACULTY OF SCIENCE AND TECHNOLOGY

MASTER'S THESIS

Study programme/specialisation: Computational Engineering	Spring/ Autumn semester, 2021.. Open / ~~Confidential~~
Author: Vegard Valberg	
Programme coordinator: Aksel Hiorth Supervisor(s): Reidar Brumer Bratvold, Aojie Hong	
Title of master's thesis: A Decision Analysis Framework for Offshore Green Ammonia Project Investments	
Credits: 30	
Keywords: offshore green ammonia, green ammonia, carbon neutral fuels, hydrogen, ammonia fuel, decision analysis, decision framework, exploratory data analysis, Monte Carlo simulation	Number of pages: 86 + supplemental material/other: 9 Stavanger, 21 June 2021 date/year

Abstract

Ammonia has great importance to our daily lives – it is used in household cleaning products and to make agricultural fertilizers. Recently it has attracted attention from the energy sector, since it can be used as a renewable, CO_2 neutral fuel, either directly or as a storage form of hydrogen (another renewable, CO_2 neutral fuel). Green ammonia production is a proven technology that uses air, water, and renewable, CO_2 neutral energy (e.g., wind, solar, or geothermal power) to generate ammonia. The entire production chain of green ammonia can be located onshore or offshore. The goal of this thesis is to generate useful insight to support the decision on whether an energy company should invest offshore green ammonia plant.

For achieving this goal, we develop a decision analysis framework for offshore green ammonia production. In this framework, we use an influence diagram to frame the decision problem. Through a literature review we identify key, relevant uncertainties and their ranges. We formulate economic models for offshore green ammonia production, use sensitivity analysis to identify material uncertainties, and perform Monte Carlo simulation to assess the economic, in terms of net present value (NPV), uncertainty of offshore green ammonia production. Based on the Monte Carlo simulation results, we develop statistical models for assessing the probability of an offshore green ammonia project being profitable (NPV > 0), given any daily production capacity and cost of an offshore platform.

We conclude that offshore green ammonia could be economically viable if certain preconditions are met (these are described later in the thesis). Therefore, it is worth carrying out further inquiries and research, as detailed elsewhere in this thesis.

This thesis develops a novel decision analysis framework for supporting a decision on whether to invest in an offshore green ammonia project, relevant and material uncertainties are identified, and a method to assess the probability of an offshore green ammonia plant being profitable.

Acknowledgements

There are several groups and individuals whose assistance was essential for the completion of this thesis. We would like to extend our heartfelt thanks to all of them.

Subsea 7, who at the height of the corona pandemic still sent representatives to Indøks Karrieredagen (the job fair held by the association for Industrial Economics students), and graciously provided the very interesting topic of this thesis.

Dr Reidar Brumer Bratvold, whose piercing questions helped clear up doubts and misunderstandings.

Dr Aojie Hong, whose review and comments on our manuscripts were invaluable in clearing up obscure passages, as well as to better organise our thoughts.

Baldur Kárason, for taking time out of his day to answer questions about an eight year old master's thesis, and whose work was of great importance for our own thesis.

The University Library at the University of Stavanger, for their ability to quickly locate and provide even the most obscure sources.

Finally, I would like to thank the many people, too numerous to name, who took time to answer quick one-off questions about their field of expertise.

Table of Contents

List of Figures

List of Tables

1. Introduction

1.1. What is Offshore Green Ammonia

Offshore refers to locating the entire ammonia production chain offshore. By green we mean that the ammonia is generated using only renewable energy (such as wind, solar, or geothermal energy). So offshore green ammonia would mean building the ammonia plant on an offshore platform, and then producing the ammonia from air and seawater, using offshore renewable energy.

1.2. Abbreviation of Offshore Green Ammonia (OGA)

The first time offshore green ammonia (OGA) is used in a subsection it will be spelled out in full, thereafter it will be abbreviated OGA. We felt this would be most convenient since we cannot be sure if a reader will go through the entire thesis in order, and we are coining OGA as an abbreviation for this thesis.

1.3. Background

For the average citizen, climate change is going from a matter of dire warnings from expert panels, to a lived experience. In a single lifespan we have witnessed increased rainfall, more extreme weather, and increasingly hotter summers. For many years there has been a general acceptance of the fact that global warming is caused by increased CO_2, and that firm and decisive action is required to stop it (Austgulen, 2012).

Increasing public interest has reached the field of energy and transportation (Pidgeon et al., 2017). We have seen official interest in alternative fuels such as hydrogen, for instance in the Norwegian Government's hydrogen strategy (Norwegian Ministry of Petroleum and Energy and Norwegian Ministry of Climate and Environment, 2020). This ties in with multiple initiatives to ensure that all personal vehicles are carbon neutral after 2025 (Samferdselsdepartementet, 2020). Likewise, efforts are underway to eliminate the carbon emissions of Norwegian ferries (Statens Vegvesen, 2020).

It has proven easier to document government initiatives than private ones, since government decisions and regulations are easily accessible to the public and in a consistent format. However, the press has already mentioned several private initiatives to develop hydrogen powered ships (Saul & Chestney, 2020; Timperley, 2020). Likewise, in Norway, the vessel Viking Energy is being fitted with ammonia fuel cells (Brown, 2020).

This was the climate in which Subsea7 decided to study the topic of offshore green ammonia (OGA). Although some experimental work is being done with an offshore refuelling station (Tollaksen, 2021) there are still many unknowns, both known unknowns and unknown unknowns.

The latter term “known unknowns and unknown unknowns” deserve an explanation, as they are very relevant to this thesis. Known unknowns are things that we know that we do not know, such as the weather next month, or the best way to build an offshore refuelling station. Unknown unknowns are things where we do not know that there is something to know. As an example, let us take the Goodyear airdock, built in 1929 in Akron, Ohio. At the time it was the largest metal structure ever built, and they took into account a variety of factors such as how the metal would expand differently depending on where the sun shone (Stuart, 1929). What they did not take into account was that the structure was large enough to cause a massive differential between outside and inside temperatures. This meant air moisture might condense inside and “rain” down. They were in the end forced to build a secondary ceiling to stop this “rain” (Van Duyne, 1941). Indoor rain in large hangars is a known issue today, but in 1929 it was an unknown unknown.

At the moment there are several competing carbon neutral fuels. To name but a few: turning captured carbon into fuels (Pearson et al., 2011); hydrogen (van Renssen, 2020); and green ammonia (Valera-Medina & Banares-Alcantara, 2020b). All of these fuels have a good many technical and economical obstacles in their way.

Certainly, green ammonia is experimental, there are only a few case studies of whether or not it can be profitable under very favourable circumstances (producing ammonia for an island where imports of diesel can be expensive) (Morgan, Manwell, & McGowan, 2014). No studies whatsoever have been made of whether OGA is technologically viable, and even the attempts to generate offshore hydrogen are still in the start-up phase (Tollaksen, 2021).

Predicting which future technology will win out can be very difficult. As any partisan of the format wars of BetaMax and VHS, or BluRay and HD DVD will tell you: The “best” technology is not necessarily the one which wins out.

In this thesis we will make some initial assumptions, these will be explained and justified further on. Key among these is that we will assume that green ammonia will be adopted as a mainstream fuel, and that onshore green ammonia is economically viable. We will also assume that OGA is technically feasible. Should any of these assumptions fail it is trivial to see that a rational decisionmaker should reject any OGA project.

With these assumptions in mind the question becomes: when should a rational green energy company should invest in an OGA project?

Though we lack knowledge we can still assign probabilities or ranges to any estimates. For any possible future event we will rarely have the true probability p of a successful outcome. Nor do we necessarily have the data necessary to calculate an estimate $\hat{p}$ from samples. However, we can always make an estimate that the true probability p is somewhere in the range $[a , b]$, in extreme situations we can say that any probability must be in the range $[0 , 1]$. Likewise, the magnitude of any value can be estimated in the same way, stating that we believe it is somewhere in the range $[a , b]$, where a and b are our estimates of the lowest and highest possible value.

The Monte Carlo method is particularly well suited for a model with both independent and dependent variables. Especially where there are wide ranges for the potential value of each independent variable. With this method we generate a number of samples. In each sample the value of every independent variable is drawn randomly from within its range. By comparing a sufficiently large number of samples we can use exploratory statistics to see which variables are more influential, and how changes in multiple variables affect the whole model.

Of course, a Monte Carlo approach requires that you have a good model. That is, you need to know what variables you need to simulate and how they will affect the model as a whole.

In some cases, we have what we strongly suspect are dependent variables, but our literature search found no models of the relationship. An example is the relationship between the size of the ammonia plant and the cost of the offshore platform. Since we found no model, we decided to treat the cost of the offshore platform as an independent variable, with a range decided on in consultation with experts.

2. Scope of the Thesis

We make the assumption that green ammonia fuel will at some future stage be viable both technologically and financially. The likelihood of this happening, and the means by which it could happen, is beyond the scope of this thesis.

Technology will mainly be treated as a black box. Those interested in an introduction as to how green ammonia can be produced can read Rouwenhorst, Krzydwa, Benes, Mul, and Lefferts (2020) "Ammonia Production Technologies". For our purposes we need not care if, for instance, we are using an **ad**sorbent or **ab**sorbent enhanced synthesis loop. In our approach what matters is the size and cost of the apparatus, as well as its energy consumption. Where applicable we will use projections from the literature as to how advancements might change cost, energy consumption, etc, in general. Further technical details are beyond the scope of this thesis.

There are key social, economic, and political factors that will influence this decision. There is an extensive literature on the economic effects of global warming (Dietz, Bowen, Doda, Gambhir, & Warren, 2018; Stern et al., 2006), how public discourse is affected (Austgulen, 2012; Pidgeon et al., 2017; Ytterstad, 2011), and so on. There are also any number of government subsidies, research grants and so on, as well as discussions of their importance (see for instance White, Lunnan, Nybakk, and Kulisic (2013)). This is obviously a very rich field of study, but the papers we were able to find were not directly helpful when it came to turning this into a model. We could do a more thorough literature search, but we do not see compelling reason to believe that this would be fruitful. Another option would be a thorough research project as to what makes a development more likely to receive support, as well as the scale of such support. The latter however would be a daunting thesis topic of its own. So, we will put most of these matters outside the scope of this thesis and rely on expert assessments and advice when it comes to working out our model.

An offshore green ammonia (OGA) project would necessarily be challenging both technically and economically. Managing such a project would involve extensive consulting with stakeholders, making complex business cases, and organizing the financing of the project itself (Gardiner, 2005). The latter aspect, financing the project, would be an immense undertaking potentially involving bonds, loans, or gaining investments from venture capitalists (Hillier, Ross, Westerfield, Jaffe, & Jordan, 2018). We will use a relevant, but very simple financial model in this thesis and not go into details as to the financing of this project.

3. Background

3.1. Efforts to Find Alternative Fuels

For decades there has been a push to reduce our reliance on fossil fuels, resulting in a series of treaties such as the United Nations Framework Convention on Climate Change (UNFCCC) (1992), the Kyoto Protocol (1997), and the Paris Agreement (2016).

Eliminating the use of fossil fuels has been part of this effort. In Norway, for instance, there has been a deliberate policy to use government action to promote the use of electric vehicles in order to reduce CO_2 emissions (Halvorsen, 2009). There have also been efforts to use batteries to power ships, an example would be the Norwegian efforts to develop electrical ferries (NRK, 2021). There have also been several other efforts to develop battery powered ships (Alnes, Eriksen, & Vartdal, 2017).

However, there are for now limits to what you can do with batteries, as both Thomas (2009) and Alnes et al. (2017) explains. These limits mean that we require other fuel sources. Although Thomas (2009) is mainly concerned with hydrogen as an alternative fuel, Alnes et al. (2017) states that the shipping industry is likely to use a portfolio of fuels in the future. Certainly, Hydrogen is already mentioned in the press (Timperley, 2020) and has been the focus of Norwegian government policy (Norwegian Ministry of Petroleum and Energy and Norwegian Ministry of Climate and Environment, 2020).

3.2. Ammonia as a Fuel

As the previous section indicates there is a definite niche for ammonia as a fuel, though even supporters of green ammonia does not claim it is a panacea for humanity’s future energy carrier needs (Valera-Medina & Banares-Alcantara, 2020b).

The history of research into ammonia as a fuel goes back a long way, during World War II there were vehicles fuelled by ammonia (De Vries, Okafor, Gutesa-Bozo, Xiao, & Valera-Medina, 2020), in 1966 the US Army tested ammonia as a helicopters fuel (Kailos, 1966), and even the X-15 rocket plane was powered by ammonia (Seaman & Huson, 2011). Today we see that Equinor’s Viking Energy supply vessel is being refitted to run on ammonia (Brown, 2020), and MAN Energy Solutions is doing research on modifying their engines to run on ammonia (Laursen, 2018).

The latter is an important point, it means that a lightly modified internal combustion engine can use ammonia as a fuel. This is a key benefit, since it would allow for a faster switch-over to a carbon neutral fuel. Though it should be noted that the most promising tests used either carbon-based fuels mixed with ammonia, or ammonia doped with hydrogen (De Vries et al., 2020). Moreover, ammonia can also be used in gas turbines (Bull, 1968), as well as boilers, and fuel cells (De Vries et al., 2020).

A key reason for ammonia's usefulness as a fuel is found in its chemical formula: NH_3. One atom of Nitrogen and three of Hydrogen. Concretely this means that ammonia can carry $106\frac{kg}{m^3}$ of hydrogen at 27°C, against $70\frac{kg}{m^3}$ for liquefied hydrogen at -253 °C (Djinović & Schüth, 2015; Valera-Medina & Banares-Alcantara, 2020a). Being easier to store and transport ammonia has the potential to help in the creation of the hydrogen economy by, among other things (Nayak-Luke, Forbes, Cesaro, Bañares-Alcántara, & Rouwenhorst, 2020; Valera-Medina & Banares-Alcantara, 2020a).

In short: Ammonia can itself be used as a fuel, or as a means to store and transport hydrogen. In the latter case it may be necessary to decompose the ammonia (e.g. separate it into hydrogen and nitrogen) which is currently a difficult process (Djinović & Schüth, 2015). It should be noted that there has been recent progress in decomposition (Lim et al., 2020), which could make ammonia an even more desirable hydrogen carrier.

3.3. Production of Green Ammonia

We want to emphasise the green part of green ammonia. Green, as in: it should be carbon neutral, environmentally friendly, and preferably rely on renewable resources and energy.

We only need three ingredients: Water, air, and some form of green energy such as wind or solar power (Sánchez & Martín, 2018a). Aside from those two we will also briefly discuss offshore geothermal power, which has the potential to give us access to an immense untapped green energy resource (Banerjee, Chakraborty, & Matsagar, 2018; Toralde, 2014)

Having accounted for our ingredients we can look at the main process of green ammonia production in Figure 3-1 (below):

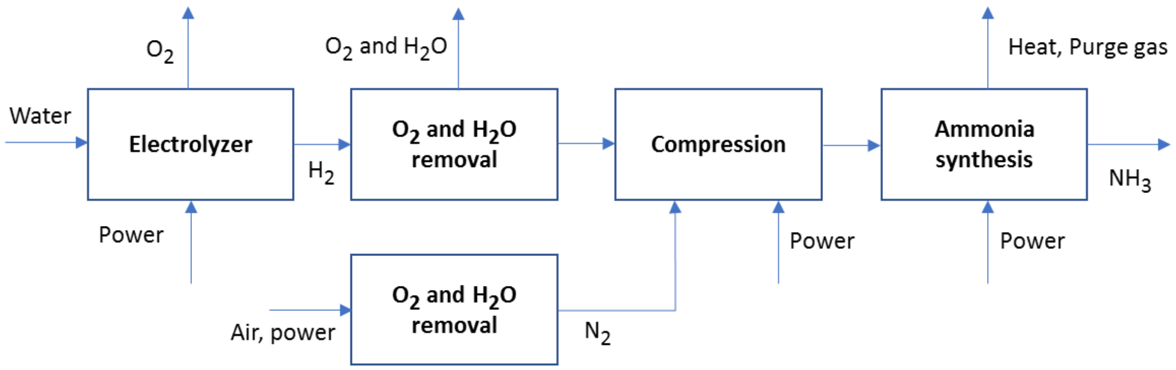

Figure 3-1 Schematic of green ammonia synthesis process with electrolysis-based hydrogen production, from Rouwenhorst, Krzydwa, et al. (2020)

In the electrolysis step water is split into hydrogen and oxygen, this requires overcoming the chemical bonds in the H_2O molecule to cause the chemical reaction:

$$2H_2O \longrightarrow 2H_2 + O_2 \qquad (3\text{-}1)$$

This step requires about 75%-90% of the total energy of the ammonia production process (Rouwenhorst, Krzydwa, et al., 2020).

Meanwhile air is being taken into an air separation unit, often a cryogenic unit, which separates nitrogen from the air. This is a known and proven process which is used on a large scale today (Rouwenhorst, Krzydwa, et al., 2020; Sánchez & Martín, 2018a). It should be noted that it is also energy intensive (Sánchez & Martín, 2018a).

All remaining oxygen and water vapor must be removed from the nitrogen and the hydrogen gasses before they are sent into the compressor (Rouwenhorst, Krzydwa, et al., 2020). After being compressed they are fed into the ammonia synthesis loop, where undesirable gasses are ejected while unreacted hydrogen and nitrogen is recycled (Sánchez & Martín, 2018a).

Although there exists any number of experimental technologies to handle all of the steps in this process, we are still dealing with a well understood process that has been used in actual industrial scale production (Rouwenhorst, Krzydwa, et al., 2020).

3.4. Offshore Renewable Energy

Offshore wind power is an industry that is still maturing, but rapid progress is made (Aspelund et al., 2019). This is confirmed by discussions with experts. Offshore geothermal power however is at the moment very much an experimental field, (Banerjee et al., 2018; Toralde, 2014) and as far as we can find there has never been even a single experimental offshore geothermal powerplant.

Aspelund et al. (2019) have shown that there has been a steady tendency towards larger wind turbines, with an ever-increasing diameter and power generation capacity. Earlier wind turbines were mounted on a bottom fixed foundation (that is fixed to the seabed), but in recent years we have seen the development of floating foundations especially as new constructions are made at greater and greater depths.

Given that our project is meant to be a self-contained offshore facility it stands to reason that it will be built on the deep seas. This is, as Aspelund et al. (2019) points out, still somewhat experimental, but has great potential in opening up unused wind resources. If it is out in the deep seas it will also not suffer from conflicts over the use of coastal waters, as mentioned by Tiller, Brekken, and Bailey (2012).

Meanwhile, as stated earlier, offshore geothermal being completely experimental means that there are few facts or figures on cost and capacity, except for Karason (2013). If it could be made to work it is however a very promising technology.

3.5. Offshore Production of Green Ammonia

Offshore green ammonia (OGA) requires that the entire production chain be offshore. This is very much on the cutting edge of technology. There have been some concepts where energy is generated onshore while the ammonia production is located on an offshore ship (Rouwenhorst, Elishav, et al., 2020). However, the only full on OGA proposal is a concept by Thyssenkrupp with both energy generation (by wind turbines) and ammonia production being fully offshore (Brown, 2018). At the time of writing we are left with pure speculation as to costs and technical difficulty.

4. Theory, Structure & Assumptions

4.1. Viability and the Price of Onshore Green Ammonia

We know that onshore green ammonia production is technologically viable, as there have been multiple proofs of concept (Armijo & Philibert, 2020; Morgan et al., 2014). The question is rather whether it is economically viable, e.g. profitable.

This is not simply a matter of whether the sum of the cashflows in and out are positive or negative. We need to take into account the time value of money (we value money now, more than potential money in the future). This is where Net Present Value (NPV) is commonly used, applying a discount rate *r* (the precise size of which is chosen by the decision maker) we sum up the cash flows in and out thus:

$$\mathrm{NPV} = \sum_{i=0}^{N} \frac{Income_{\mathrm{i}} - Expenses_{i}}{(1+r)^{i}} \tag{4-1}$$

Where i is the year, starting with $i = 0$ for the current year.

If we grant that the sale and purchase of electricity evens out, e.g. that over a year it has no economic effect, then only the price of ammonia $P_{onshore}$ will act as an income, if we assume no economic profit (e.g. NPV=0) we get the equation:

$$0 = -InitialExpense + \sum_{i=1}^{N} \frac{Income_{\mathrm{i}} - Expenses_{i}}{(1+r)^{i}} \tag{4-2}$$

$$Income_{\mathrm{i}} = P_{onshore} \times AnnualProduction \tag{4-3}$$

InitialExpense is the proportion of capital expense (CapEx) that needs to be paid up front (if any).

Expenses$_i$ are all annual expenses for the year *i*, whether from servicing loans or operational expenses (this will be explained further on).

Since *AnnualProduction* is constant for any one sample all that remains is to find the lowest price, $P_{onshore}$, fulfilling the criteria NPV=0. By definition we now have a price for which an onshore green ammonia plant is viable as far as the NPV criteria is concerned.

For further details we would like to direct your attention to section 4.4.2.

The reason this is important is not that we need the price $P_{onshore}$ to calculate the market price of offshore green ammonia (OGA) (see section 4.6.8. and equation (4-32)).

4.2. Technology as a "Black Box"

As mentioned in section 2. Scope of the Thesis, technology will mostly be treated as a black box. Our decision to do so was determined by two factors:

1. We are not chemists, nor experts in production techniques, or offshore engineering.
2. For the purposes of this thesis the exact technical details are not important.

As such any discussion of technology will be very limited.

4.3. Concerning Subsidies

In the background (section 3.1.) we mentioned government attempts to encourage green energy and energy carriers. It should be common sense that subsidies, if they are large enough, can make any project profitable.

As White et al. (2013) points out: if government promises are seen as unreliable this leads to uncertainty, which is something that risk adverse investors dislike. This may lead to projects prematurely being shut down, or fail to be launched altogether. If on the other hand a government commits to its promises, any investors will include promised subsidies or aid in their calculations.

In this thesis we have chosen to abstract away the issue of investor confidence in government assurances. Thus, the subsidies, if any, are simply factored into the NPV.

4.4. Influence Diagrams

For readers interested in a more detailed explanation of influence diagrams and the related concept of decision trees we recommend Bratvold and Begg (2010) *Making Good Decisions*. So, we will only give the quickest, most barebones explanation.

Influence diagrams are a very powerful way of illustrating the relationships between various types of nodes, which are connected by relevance arrows. The basic symbols are explained in Table 4-1 below:

Name	**Explanation**	**Symbol**
Decision node	A decision node marks a decision that needs to be made. Such a decision is a definite commitment that cannot be easily changed afterwards.	
Uncertainty node	An uncertainty node marks the unknown future state of some relevant factor. An example might be the efficiency of some new technology, or a government subsidy.	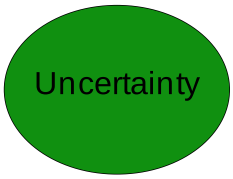
Value node	A value node is some definite value whose relationship with other nodes is known. It may be affected by other nodes (such as NPV), or simply stand by itself (such as the lifespan of the project).	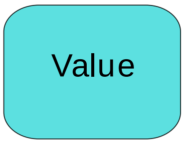
Special node	A special node in this influence diagram stands for a collection of nodes and/or relevance arrows that are omitted in order to avoid excessive clutter in our diagrams.	
Relevance arrow	A relevance shows that one node is connected to or influences another. The direction of the arrow indicates the direction of the influence.	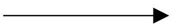

Table 4-1: Explanation of the concept of nodes and relevance arrows for influence diagrams.

4.4.1. Influence Diagram for Offshore Green Ammonia (OGA)

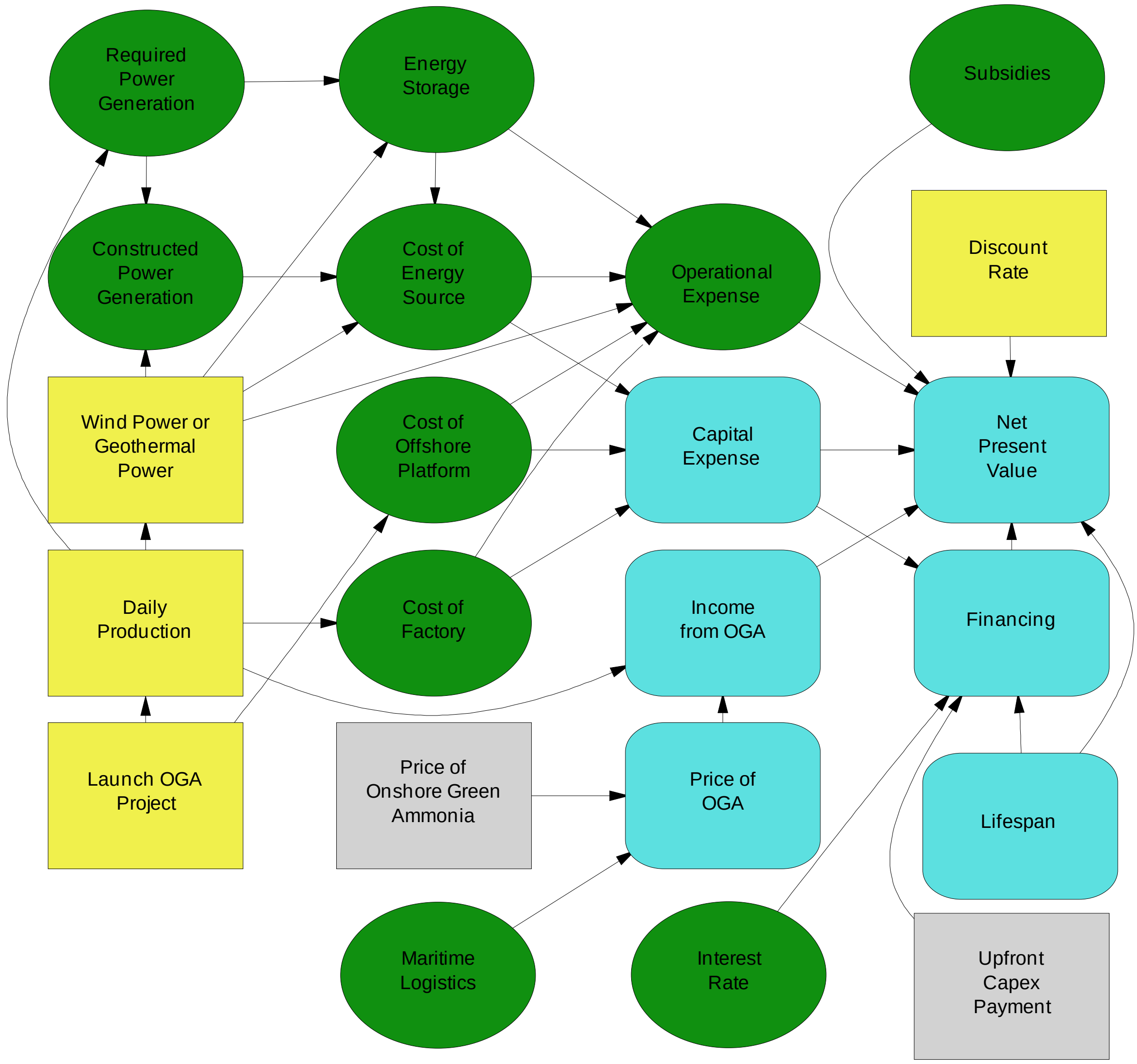

Figure 4-1: Influence diagram for offshore green ammonia (OGA)

Please see Table 4-2 below for an explanation of the various sections. Note that we would begin at the decision (yellow) marked "Launch OGA Project".

4.4.2. Influence Diagram for the Price of Onshore Green Ammonia

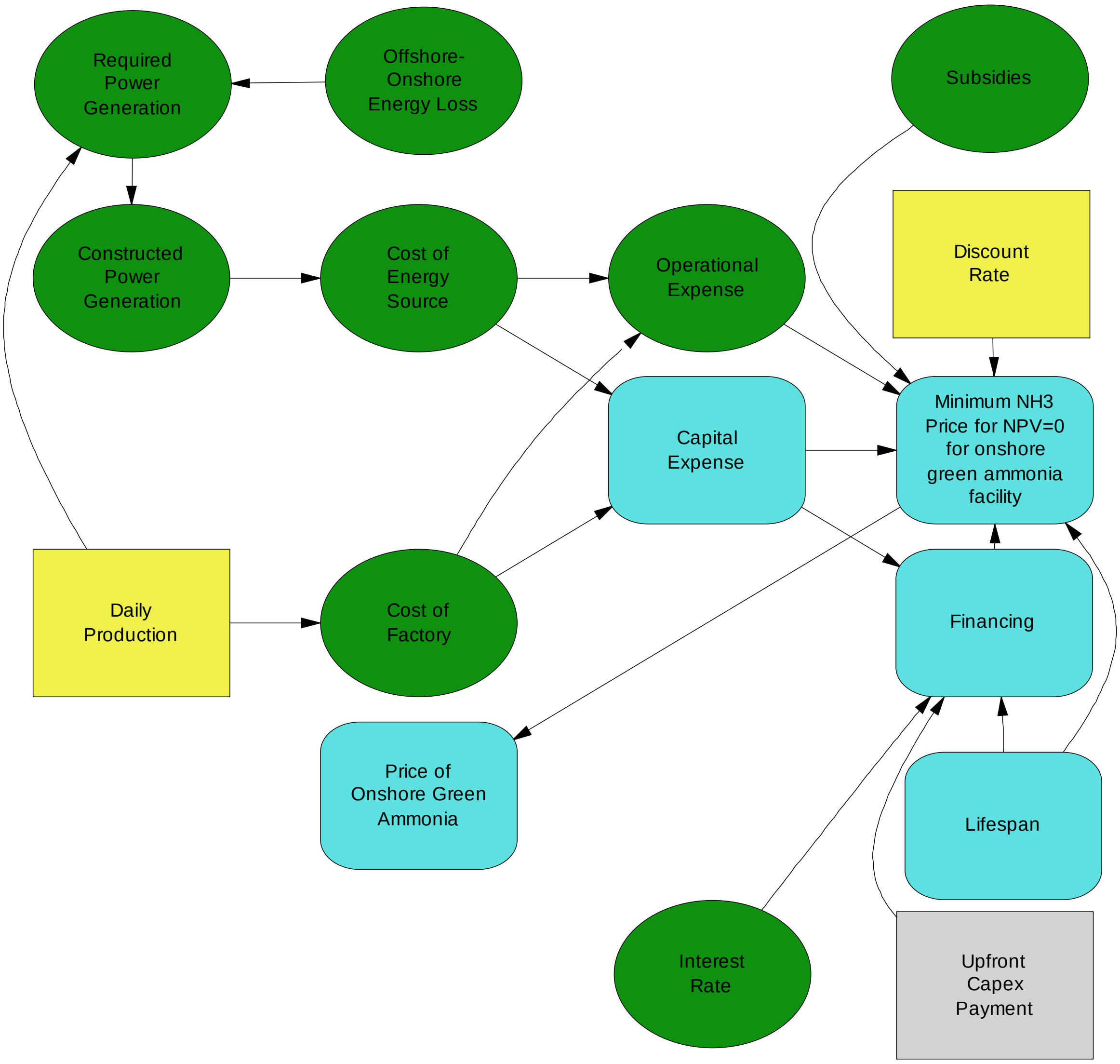

Figure 4-2:Influence diagram for the price of onshore green ammonia

This influence diagram would normally be part of the former diagram, but there we marked it as a special node to avoid excessive clutter. Again please see Table 4-2 below for an explanation of the various sections.

4.4.3. Explanatory Table

Name	Type	Description
Launch OGA Project	Decision	Do we invest in the offshore green ammonia (OGA) project, or decline to make any investment?
Daily Production	Decision	Daily ammonia production in tons.
Discount Rate	Decision	Discount rate for NPV calculations.
Wind Power or Geothermal Power	Decision	A decision as to whether, or not we should use wind power or geothermal power.
Price of Onshore Green Ammonia	Special	The price of green ammonia produced at an onshore facility, if the NPV of said facility is zero.
Upfront Capex Payment	Special	Proportion of total capital expense that needs to be paid in advance. As opposed to the capital expense paid for over time, whether by loans or other financial instruments. This is marked as a special node to denote the complexity of the issue (which would be influenced by several nodes).
Constructed Power Generation	Uncertainty	The amount of power generation that needs to be built to operate the platform.
Cost of Energy Source	Uncertainty	The cost of the energy source (wind or geothermal).
Cost of Factory	Uncertainty	The cost of the factory itself.
Cost of Offshore Platform	Uncertainty	The cost of the offshore platform.
Energy Storage	Uncertainty	The amount of energy storage required per MW or required power generation.
Interest Rate	Uncertainty	The interest rate for any loans etc.
Maritime Logistics	Uncertainty	How the market prices the benefits of improved maritime logistics due to an offshore refuelling station.

Name	Type	Description
Offshore-Onshore Energy Loss	Uncertainty	The proportion of energy that is lost in transfer from an offshore wind turbine facility to an onshore factory.
Operational Expense	Uncertainty	The operational expense depending on capital expense and other factors.
Required Power Generation	Uncertainty	The amount of power that needs to be supplied in order to run the facility.
Subsidies	Uncertainty	Potential government subsidies.
Capital Expense	Value	Capital expense of the project.
Financing	Value	Various costs (interest, repayment etc) due to the scheme picked for financing the project. This includes any loans or other financial instruments used to raise funds for capital expense.
Income from OGA	Value	Income from OGA.
Net Present Value	Value	Net Present Value of the OGA project.
Price of OGA	Value	Price of OGA given the maritime logistics.

Table 4-2: Explanatory table for influence diagram

4.5. Independent Variables

The ranges given for each independent variable indicate uncertainty. This uncertainty can be because of: a lack knowledge; an outcome that is by its nature random; or because it depends on decisions not yet made. For instance r_{discount} (our discount rate) would be chosen by our decision maker, but we do not know what choice they will make. So, to us it is an uncertainty.

What we mean by $N \in [a, b]$ is that for the purposes of our thesis N is assumed to be in the specified range. Further, in each iteration of the Monte Carlo simulation the number N will be a sample drawn from a uniform distribution with the specified upper and lower bounds.

Variable	Explanation	Value	Unit
CapExPlatform	Cost of the offshore platform	$N \in [0\,, 25] \times 10^9$	€
CapExUpfront	Proportion of CapEx that needs to be paid up front	$N \in [0\,, 0.25]$	None
CapFactor	Capacity Factor of the wind turbines	$N \in [0.4\,, 0.8]$	None
CCWind	Change in cost of windmills	$N \in [0.75\,, 1]$	None
CostGeoMW	Cost of geothermal energy pr MW	$N \in [4.6\,, 12.4] \times 10^6$	€
ESCostMW	Cost of energy storage needed for offshore platform per MW windpower	$N \in [50\,, 250] \times 10^3$	€
LandPwrLoss	Efficiency losses due to being onshore	$N \in [0\,, 0.2]$	None
Lifespan	Lifespan of project	25	Years
OpNMainRateES	Operations and maintenance (Op.&Main.) rate for the energy storage	$N \in [0.01\,, 0.05]$	None
OpNMainRateFac	Op.&Main. rate for the factory	0.045	None
OpNMainRateGeo	Op.&Main. rate for geothermal power	$N \in [0.001\,, 0.025]$	None

Variable	Explanation	Value	Unit
OpNMainRateOff	Op.&Main.rate for the offshore platform	$N \in [0.01\,, 0.05]$	None
OpnMWindMW	Main. of windturbines in € per MW per year	110×10^3	$\frac{€}{\text{year} \cdot \text{MW}}$
$\mathrm{p}_{\mathrm{SubAnnual}*}$	Probability of an annual subsidy (from year 1)	$N \in [0\,, 1]$	None
$\mathrm{p}_{\mathrm{SubInit}*}$	Probability of an initial subsidy (in year 0)	$N \in [0\,, 1]$	None
ProdDays	Days with full production	330	Days
PwrNH3Dly	Power (in MW) req. pr ton of NH_3 per day	$N \in [0.324\,, 0.579]$	$\frac{\text{MW}}{\text{ton} \cdot \text{day}}$
$\mathrm{r}_{\mathrm{discount}}$	Discount rate	$N \in [0.06\,, 0.12]$	None
r_{loan}	Interest rate for loans	$N \in [0.015\,, 0.05]$	None
$\mathrm{SubAnnualProp}_*$	Scale of initial subsidy (from year 1 on)	$N \in [0\,, 1]$	None
$\mathrm{SubInitProp}_*$	Scale of initial subsidy (year 0)	$N \in [0\,, 1]$	None
TonsPerDay	Tons of ammonia produced per day	$N \in \left\{ \begin{matrix} x \in \mathbb{Z}: \\ x \in [250\,, 2000] \end{matrix} \right\}$	$\frac{\text{ton}}{\text{day}}$
xPrice	Premium that the shipping industry is willing to pay for offshore delivery	$N \in [1\,, 2]$	None

Table 4-3: Independent variables and their typical values or ranges.

Note that TonsPerDay is always an integer, as indicated by $x \in \mathbb{Z}$.

4.6. NPV

4.6.1. Calculating the Capital Expenses (Exclusive of Platform Cost)

To produce ammonia, we need an ammonia factory. In this thesis we will treat the various facilities for desalination, electrolysis, and ammonia synthesis as a single package. Morgan et al. (2014) gave a formula for calculating the cost of such a facility based on its daily production in tons of ammonia, and this formula was simplified by Rouwenhorst, Krzydwa, et al. (2020). For convenience we will be using that simplified version:

$$CapExFactory = €3.3 \times 10^{6} \times TonsPerDay^{0.6} \tag{4-4}$$

Next, we have PwrNH3Dly, which is the power in MW required to produce one ton of ammonia per day. We have found GJ figures from Rouwenhorst, Krzydwa, et al. (2020) and adapted the approach of Morgan, Manwell, and McGowan (2017) by converting this to MW required for daily production.

To deal with the fact that wind is not constant we use what is known as the Capacity Factor (CapFactor):

$$CapFactor = \frac{Average\ Power\ Production}{Rated\ Power\ Production} \tag{4-5}$$

We know that in the real world the capacity can vary between 40%-60% depending on where the wind turbine is positioned (Armijo & Philibert, 2020). It is also known that the capacity factory is likely to rise as a result of technological developments (Wiser et al., 2016). Our estimate of 40%-80% is somewhat unrealistic on the upper end, even with technological developments. We chose a generous upper limit to ensure that all likely future developments are contained within the limits.

An effect of this is WindOutput, which is how many MW of nominal capacity we need in order to ensure that on average we have the required power:

$$WindOutput_{offshore} = \frac{TonsPrDay \times PwrNH3Dly}{CapFactor} \tag{4-6}$$

In the case of an onshore green ammonia facility receiving electricity from offshore.

We must account for energy loss during transition, which has been discussed by, among others, Aspelund et al. (2019). We account for this with the variable LandPwrLoss, which is the loss of power during transition, giving us:

$$WindOutput_{onshore} = \frac{TonsPrDay \times PwrNH3Dly}{CapFactor \times (1 - LandPwrLoss)} \tag{4-7}$$

The cost of wind turbines in the future is somewhat uncertain. After reading Wiser et al. (2016) and consulting with experts we decided that the cost per MW of wind turbines could vary by approximately 25%. This was the value used to determine CCWind (see Table 4-3).

We found our default cost per MW in Kikuchi and Ishihara (2019) and will take it as our norm, giving us the cost of wind turbines per MW as:

$$CostWindTurbineMW = 3.8 \times 10^6 \times CCWind \tag{4-8}$$

We then have the capital expense (CapEx) of the wind turbines:

$$CapExWind = CostWindTurbineMW \times WindOutput \tag{4-9}$$

As we mentioned earlier the reason there is a capacity factor is that we cannot fully rely upon the wind. As discussed by Lund and Paatero (2006) as well as Holttinen (2005) energy storage may be required in order to level the energy load. However, it is hard to find a good estimate of the cost of this energy storage, especially as different types of storage (flywheel, batteries, etc) have different uses and qualities (Lund & Paatero, 2006). Our estimate of the costs comes primarily from Lund and Paatero (2006), with brief consultations with experts. This then is the ESCostMW (Energy Storage Cost per MW):

$$ESCostMW \in [50{,}250] \times 10^3 \tag{4-10}$$

Amount is in Euros (€). From this we get a capital expense for energy storage (CapExES):

$$CapExES = ESCostMW \times PwrNH3Dly \times TonsPrDay \tag{4-11}$$

Unlike wind power, geothermal power is reliable and consistent over time (Banerjee et al., 2018; Toralde, 2014). However, we still need to account for the cost of building an offshore geothermal powerplant, and for this the only good cost-estimate that we were able to find was Karason (2013). Who estimated that the cost was between US$4968 and US$6624 per kW.

Since this estimate was in US$ we converted it into Euros using the average exchange rate of 2013. Rounding off and adding a 10% safety margin we fund a range between €4.6×10^6 and €6.2×10^6 per MW.

This gives us the following formula for the capital expense for geothermal power (CapExGeoPwr):

$$CapExGeoPwr = CostGeoMW \times PwrNH3Dly \times TonsPrDay \tag{4-12}$$

4.6.2. Calculating the Capital Expense of the Offshore Platform

There are no easily accessible studies on how the weight, volume and floor area of equipment affects platform cost. Nor, for that matter, is there much data on the weight, volume, and floor area needed for various sizes of ammonia factories.

This means that we are in one sense flying blind. However, as mentioned elsewhere, one can always estimate a range of possible values. Ideally, we would use the cost of oil platforms (perhaps without drilling equipment) as a reference for the floor and the ceiling of our range. We soon found that there is an enormous range of costs, and as stated elsewhere, we do not know how large of an ammonia plant can be fitted onto any given platform. Nor, for that matter, are we aware of the operations and maintenance cost of an offshore platform, or how this relates to their capital expense. Neither our literature search, nor communication with experts were able to provide any assistance.

Therefore, we will use another approach.

Looking at the floor of our range we will set it at €0. There are two reasons for this, first it seems intuitive that the price of the platform cannot dip below that point. Second, having the range start at 0 makes future analysis far more convenient.

The ceiling of our range is a more difficult matter. However, it seems clear (as shown elsewhere) that past a certain point there is little hope of the project being profitable. That is, in the real world the decision maker should simply reject the project should the platform cost go beyond this. From our preliminary studies that point is €25×10^9, which will be the ceiling of our range.

Therefore (as also shown in Table 4-3), the range of the cost of the platform is set as:

$$CapExPlatform \in [0\,,25] \times 10^9 \qquad (4\text{-}13)$$

4.6.3. Total Capital Expense (TCE)

Total Capital Expense (TCE) for offshore wind and geothermal:

$$TCE_{wind} = CapExFactory + CapExPlatform + CapExWind + CapExES \qquad (4\text{-}14)$$

$$TCE_{geo} = CapExFactory + CapExPlatform + CapExGeoPwr \qquad (4\text{-}15)$$

4.6.4. Calculating the Operational Expenses

For Operations and Maintenance Cost for Wind Turbines per MW (OpnMWindMW) we choose to use the figure of €1100 per kW (or €110 000 per MW) as per Kikuchi and Ishihara (2019). The reason for using is a set sum is that our literature search got a very limited result, so we are using the one credible source we could find.

This gives a total Operations and Maintenance Cost for Wind Turbines (OpNMWind):

$$OpNMWind = WindOutp \times OpnMWindMW \tag{4-16}$$

For the rest of the annual operations and maintenance costs we will be using some percentage of the capital expense of that component. In the case of the ammonia factory itself we have the 4.5% annual rate found in Demirhan, Tso, Powell, and Pistikopoulos (2019), and for the rest we are making a best estimate extrapolating from Morgan et al. (2017), Sánchez and Martín (2018b), and Demirhan et al. (2019).

See Table 4-3 for explanations of independent variables.

$$OpNMFactory = CapExFactory \times OpNMainRateFactory \tag{4-17}$$

For Operations and Maintenance cost for Geothermal Power (OpNMGeo) we get:

$$OpNMGeo = CapExGeoPwr \times OpNMainRateGeo \tag{4-18}$$

For Operations and Maintenance cost for Energy Storage (OpNMainES) we get:

$$OpNMainES = CapExES \times OpNMainRateES \tag{4-19}$$

For Operations and Maintenance cost for the platform itself (OpNMainES) we get:

$$OpNMainPlatform = CapExPlatform \times OpNMainRateOff \tag{4-20}$$

4.6.5. Total Operational Expense and Maintenance (TotalOpNMain)

$$\begin{aligned} TotalOpNMain_{wind} \\ &= OpNMainPlatform + OpNMFactory \\ &+ OpNMWind + OpNMainES \end{aligned} \tag{4-21}$$

$$\begin{aligned} TotalOpNMain_{geo} \\ &= OpNMainPlatform + OpNMFactory \\ &+ OpNMGeo \end{aligned} \tag{4-22}$$

4.6.6. Financing the Project

Financing and financial structure is a key issue for the planners of any major project (Hillier et al., 2018). The Total Capital Expense is likely funded partly by equity and debt financing. The difference between the two are quite important for a corporation as a whole (Hillier et al., 2018). However, in this thesis we are not interested in whether or not our project is to be handled as a project company, financed by venture capital, or through loans.

Since we are mostly interested in comparing three opportunities in the same field (onshore green ammonia with offshore wind turbines, offshore green ammonia (OGA) with offshore wind turbines, and OGA with geothermal power) we will use a greatly simplified financial model.

In our model we assume that there is a year 0 up front payment somewhere between 0% and 20%, while the rest of the capital expense is covered by a loan. That is:

$$InitialExpense = TCE \times CapExUpFront \tag{4-23}$$

Where TCE is Total Capital Expense and CapExUpFront is the proportion of capital expense that must be paid up front (also see Table 4-3).

And a loan sum of:

$$LoanSum = TCE \times (1 - CapExUpFront) \tag{4-24}$$

And we find the annual Loan Repayment by:

$$LoanRepayment = \frac{LoanSum \times rl \times (1 + rl)^{Lifespan}}{(1 + rl)^{Lifespan} - 1} \tag{4-25}$$

Where *rl* is the annual interest rate for the loans (also see Table 4-3)

4.6.7. Calculating Subsidies

Since we are uncertain of both the likelihood and the size of any subsidies, we are operating with two variables. In Table 4-3 we see the range of both. We now have a random value *D* such that:

$$D_* \in [0,1] \tag{4-26}$$

And this gives us:

$$InitialSubsidy = \begin{cases} SubInitProp \times InitialExpense, for\ D \leq p_{subinitial} \\ 0 \qquad\qquad\qquad\qquad\qquad\qquad , for\ D > p_{subinitial} \end{cases} \tag{4-27}$$

$$AnnSubsidy = \begin{cases} SubAnnProp \times LoanRepayment, for\ D \leq p_{subannual} \\ 0 \qquad\qquad\qquad\qquad\qquad\qquad , for\ D > p_{subannual} \end{cases} \tag{4-28}$$

Note that, as we will get into in the next chapter, we are able to vary these probabilities during the actual simulation.

4.6.8. Calculating the NPV

We find the NPV by the formula

$$NPV = -InitialExpense + InitialSubsidy + \sum_{i=1}^{N} \frac{(P_{actual} \times AnnProduction) + AnnSubsidy_i - AnnExpenses_i}{(1+r)^i} \tag{4-29}$$

Where we have that:

$$AnnProduction_i = ProdDays \times TonsPrDay \tag{4-30}$$

$$AnnExpenses_i = LoanRepayment_i + TotalOpNMain_i \tag{4-31}$$

$$P_{actual} = xPrice \times P_{onshore} \tag{4-32}$$

See section 4.1. for an explanation of $P_{onshore}$.

P_{actual} is the price that the market is willing to bear for offshore delivery of green ammonia.

4.7. Decision Making Criterion

In deciding on the decision-making criteria, we were aware of a variety of potentially important factors, which are mentioned in 2. Scope of the Thesis, but we decided to exclude them from this thesis. We also gave some thought to using a Profitability Index $\left(\frac{NPV}{Total\ Capital\ Expense}\right)$, which would make it easier to compare different projects.

However, in the end we decided to listen to Occam (of Occam's razor), in that "entities should not be multiplied without necessity", or in our case we should not consider additional projects without a good reason to do so. So, our decision is between investing in offshore green ammonia (OGA), or not investing at all.

We chose expected NPV as our decision-making criterion. It is generally well understood by decision makers, and we can narrow it down to being either positive or negative.

If expected NPV is positive then the decision maker should approve the project, otherwise they should not approve it.

5. Simulation Model and Method of Analysis

5.1. Carrying out the Monte Carlo simulations

Our Monte Carlo simulation was implemented as a Python script. The structure is as described in section 4.4. to 4.6.8. Note that all the values in Table 4-3 could be varied as needed, either set to a new range, or set to a specific value.

Our initial run, using default ranges for all variables (including subsidies), generated a 10^6 sample training dataset. We also generated a 10^6 sample test dataset.

Afterwards we generated the No Subsidies set, where all subsidies were disabled (the probability of subsidies were set to zero). This was also a 10^6 sample training dataset, with a 10^6 sample test dataset.

The bulk of our tests were carried out on these datasets, but a few smaller, specialized datasets were generated to examine specific aspects of our model. These will be described as necessary.

5.2. Sensitivity Analysis

Our Python script included the ability to do a sensitivity analysis. This was done by setting each independent variable (see Table 4-3) in turn to its high, low and medium (halfway between high and low) values, while keeping the values of the other independent variables at medium.

5.3. Exploring Statistical Relationships

This section will provide a brief overview of our statistical approach.

After completing the initial run of simulations various patterns began apparent as we analysed the data gathered. In order to carry out this analysis we used a variety of python and R scripts (R being a statistical programming language), as well as excel workbooks (for generating graphs and figures).

Since NPV can be defined as either being positive or negative, we found it useful to treat it as a binary variable. We then carried out statistical exploration in order to determine how variables in the model affected the probability of a positive or negative NPV.

5.3.1. Multivariable Polynomial Regression

A key aspect of our approach is the use of linear regression, in particular with binomial models and generalized linear models (applied by way of R). For more on the topic see Dobson and Barnett (2018). What we were primarily interested in was $P(NPVpos|\boldsymbol{X})$ where $\boldsymbol{X}$ is a set of values for some relevant variable(s). $NPVpos$ means NPV is positive. This required us to use R's "predict" function, which allows you to extract such probabilities in the standard form of:

$$p = \frac{1}{1 + \exp(-\boldsymbol{x}'\boldsymbol{\beta})} \qquad (5\text{-}1)$$

Where *p* here is the probability of a successful experiment (positive NPV).

This is also closely related to the mean function for a binomial distribution. Which is to say that for sufficiently large number of experiments (*N*) with a given set of $\boldsymbol{x}'$ we would expect that $p = \frac{n_{success}}{N}$.

In some cases we were interested in predicting the precise value of a variable, such as for instance NPV. In this case we would have a normal linear model, predicting a value *y* such that:

$$y = \boldsymbol{x}'\boldsymbol{\beta} + \epsilon \qquad (5\text{-}2)$$

Where ε is the irreducible error in any prediction. $\boldsymbol{x}$ is a vector of explanatory variables, while $\boldsymbol{\beta}$ is a vector of parameters (Dobson & Barnett, 2018). These parameters have been fitted, to make the response as accurate as possible (at least to the training dataset). It should be clear that $\boldsymbol{x}$ could contain multiple variables, some of which could be raised to a polynomial degree.

That is for a simple linear regression with *j* variables we'd have:

$$\boldsymbol{x}'\boldsymbol{\beta} = \beta_0 + \beta_1 x_1 + \cdots + \beta_j x_j \qquad (5\text{-}3)$$

For a polynomial regression with *j* variables raised to the *i*th degree we would have:

$$\boldsymbol{x}'\boldsymbol{\beta} = \beta_0 + \beta_{11} x_1 + \beta_{12} x_1^2 + \cdots + \beta_{1i} x_1^i + \cdots + \beta_{j1} x_j + \cdots + \beta_{ji} x_j^i \qquad (5\text{-}4)$$

But we could also have an unbalanced set of polynomials, such as one example we will see further into the thesis, where x_1 is raised to a 4^{th} degree polynomial and x_2 to a 6^{th} degree polynomial:

$$\boldsymbol{x}'\boldsymbol{\beta} = \beta_0 + \beta_{11}x_1 + \cdots + \beta_{14}x_1^4 + \beta_{21}x_2 + \cdots + \beta_{26}x_2^6 \tag{5-5}$$

We should quickly note that both p and y would count as a response, while predictors would be each variable and its powers (so variables $x_j, x_j^2, \ldots, x_j^i$ would be i different predictors).

5.3.2. General Procedure for picking the best model

Let us begin with the following flowchart:

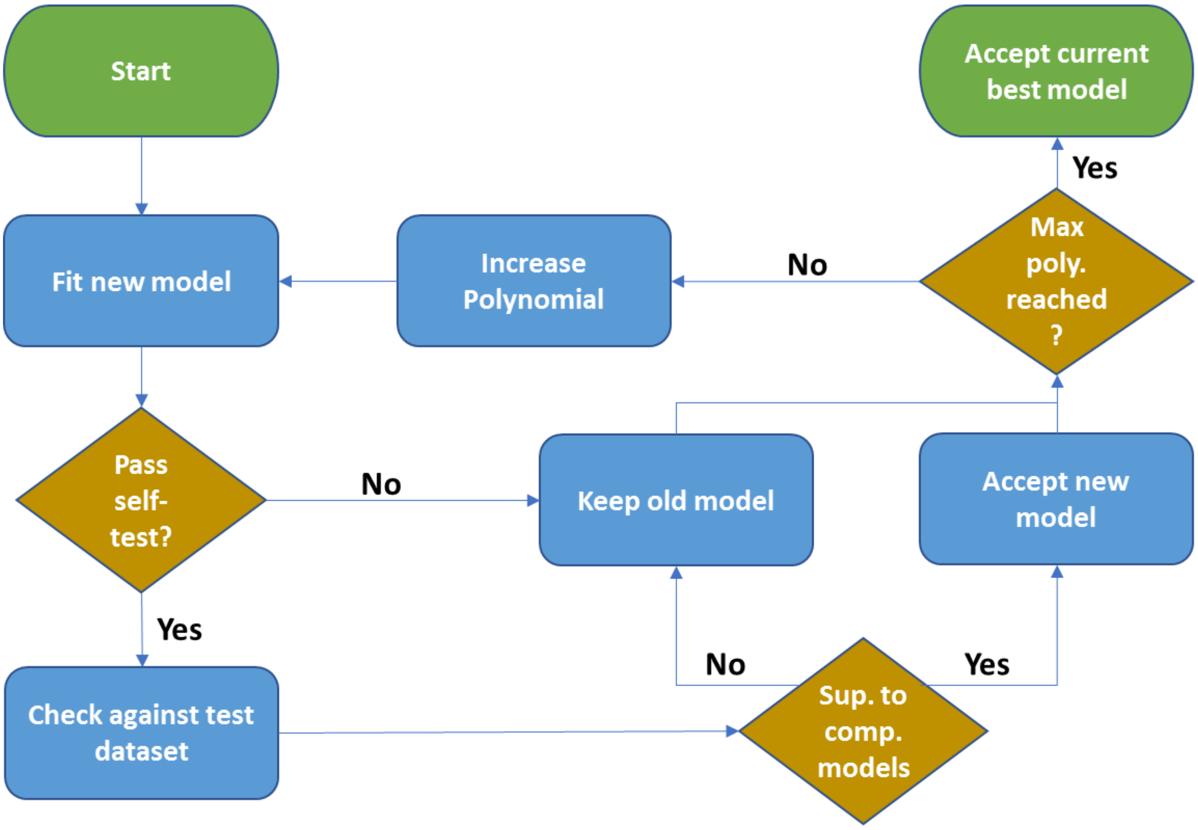

Figure 5-1: Flowchart of process for picking best polynomial model

An explanation of the symbols can be found in Table 5-1 below.

Symbol	Type	Description
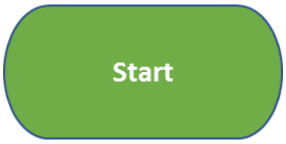	Start/ Terminal	**Start** We start the process when we want to fit a new model to a training dataset. We have already decided on the training set and what sort of model (equation (5-1) or (5-2)) we want.
	Process	**Fit new model** Fit new polynomial model starting with a 1st degree polynomial for all x_j (where in our case $j \in \{1\ ,2\}$ or $j \in \{1\ ,2, 3\}$). Then updated as according to "Increase Polynomial" (see below).
	Decision	**Pass self-test?** We check that all the coefficients (a measure of the strength of the relationship between the response and the predictors) have: $$P(Z > \|z\|) < 0.05.$$ That is less than a 0.05 probability that the relationship is spurious. We also check if the new model has superior Akaike Information Criterion (*AIC)* or R^2 (depending on which type of statistical model we are using) to the older one. See section 5.3.3. for an explanation of *AIC* and R^2. If the older model is better the new model fails the self-test.
	Process	**Check against test dataset** Once the model has passed its self-test we check how it does against a test dataset. Depending on what sort of statistical model we either check R^2 or the Brier Score (*BS*). See section 5.3.3. for an explanation of the Brier Score.

Symbol	Type	Description
Sup. to comp. models	Decision	**Superior to competing models?** Is the new statistical model superior (in terms of R^2 or *BS*) to the previous models? If so yes, if not no.
Keep old model	Process	**Keep old model** Keep the old model and reject the new one.
Accept new model	Process	**Accept new model** Accept the new model and reject the previous best model.
Max poly. reached ?	Decision	**Maximal polynomial reached?** When we fit our statistical models, we decide beforehand on the highest polynomial degree we will test. This checks if we have reached that degree or not.
Increase Polynomial	Process	**Increase polynomial** Increases the polynomial degree of one predictor (x_1, x_2 or x_3) by one. For the two predictor case imagine that AB are two digits, where A is the polynomial degree of x_1 and B the polynomial degree of x_2. Then like an old-fashioned odometer it’d go: 11-12-…15-16-21-22-…-25-25-31-…-66. (Since we do not check past the 6th degree). Same principle applies for the three predictor case. This new polynomial degree is then used to fit the next statistical model.
Accept current best model	Start/ Terminal	**Accept current best model** We accept the current best model (for the given dataset and assumptions) as the one that will move forward.

Table 5-1: Explanation of terms for the model selection flowchart.

5.3.3. Akaike Information Criterion (AIC), R^2, and Brier Score (*BS*)

The Akaike Information Criterion (*AIC*) is a goodness of fit statistic based on the log-likelihood function, with adjustment for the number of parameters estimated and for the amount of data. A small value of the statistic indicates that the model fits well (Dobson & Barnett, 2018). When comparing several models on the same data and with the same response variable we view a smaller *AIC* to indicate a better fit. Since we are using the glm function in R (since R can only treat a binomial problem as a Generalized Linear Model) the *AIC* is the best way to indicate goodness of fit without testing the model against training data.

R^2 or adjusted R^2 is a measure of how much of the variation in a data set which is explained by the model. In our case we can calculate the R^2 when we use a linear model to calculate the value of some response variable (for instance NPV). A high R^2 is an indication of a good fit.

Brier Score or *BS*, from Brier (1950), is a strictly proper scoring rule for classifiers. By strictly proper we mean that we get the best results if, and only if, we accurately predict the true probabilities. A classifier is a model where any observation must be assigned to a set number of classes (such as NPV being positive or negative).

Since we only have two classes the Brier Score can be expressed as:

$$BS = \frac{1}{N}\sum_{i=1}^{N}(f_i - E_i)^2 \qquad (5\text{-}6)$$

Where f_i is the calculated probability of a successful result, while E_i is 1 for an actual success and 0 for a failure. Here *N* is the number of samples in the dataset to be tested.

Note, whenever we used the Brier Score it was calculated by applying our model to a test dataset.

5.3.4. Area Under Curve for Receiver Operating Characteristic (AUC-ROC)

The ROC curve is a popular and well-known statistical measurement, which was originally developed during WWII by radar operators as a way to separate signal from noise, which is where the name Receiver Operating Characteristics comes from. It is a graphical method most useful in evaluating the performance of binary classifiers.

Two key concepts that we need to remember is True Positive Rate (TPR) and False Positive Rate (FPR) defined thus:

$$TPR = \frac{TruePositives}{TruePositives + FalseNegatives} \tag{5-7}$$

$$FPR = \frac{FalsePositives}{FalsePositives + TrueNegatives} \tag{5-8}$$

Our statistical models assign to every sample a probability (*p*) of being positive (e.g. positive NPV). Before we can calculate the *TPR* and *FPR* we must decide upon a threshold (*T*), above which we classify the sample as positive, and below which we classify it as negative. Once we have done this for every single sample in our dataset we can calculate both *TPR* and *FPR*.

We repeat this procedure for any number of thresholds (*T*) in the range [0 , 1]. Let us illustrate the process with a flowchart:

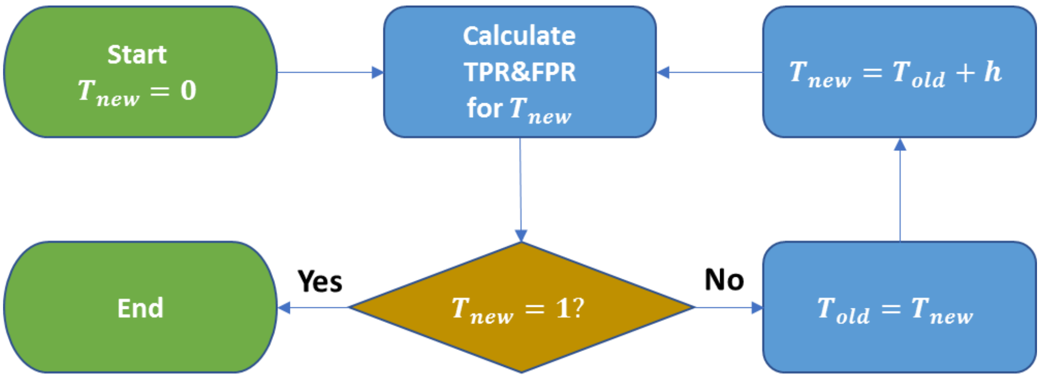

Figure 5-2: Flowchart for TPR&FPR calculations for AUC-ROC chart. Here h is a very small number.

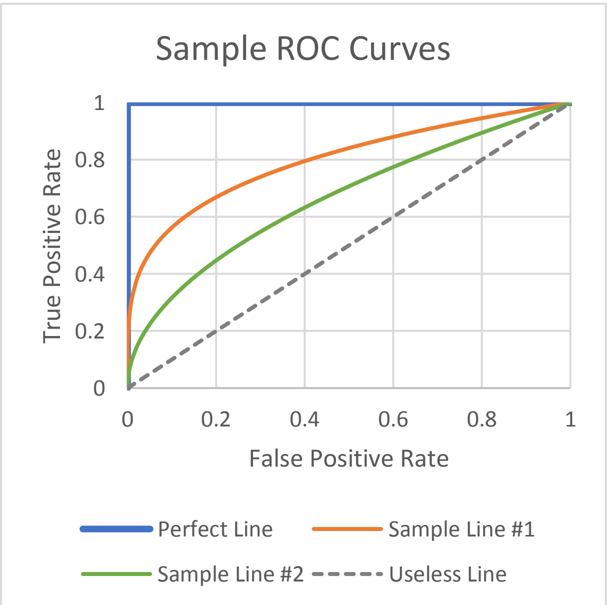

Figure 5-3: Sample ROC Curves

If *h* was an infinitesimal we would now have an infinite number of *TPR*,*FPR* pairs. If we were to place them on a scatterplot they would then form a line going in a curve from the lower left corner to the upper right. If we merely calculate a large number of points and link them up we shall, however, reach a good approximation of this line.

Figure 5-3 shows a set of sample *ROC* curves which illustrate the principle.

Note the curve labelled "Useless Line", the reason it is called such can be gleaned from "Introduction to ROC analysis" by Fawcett (2006):

> Since the AUC is a portion of the area of the unit square, its value will always be between 0 and 1.0. However, because random guessing produces the diagonal line between (0, 0) and (1, 1), which has an area of 0.5, no realistic classifier should have an AUC less than 0.5.

In short the useless line has an Area Under Curve (*AUC*) of 0.5 and is what we would expect from random guessing. The ideal *ROC* curve is something like the Perfect Line, which has an *AUC* of 1. Meanwhile Sample Line #1 and #2 have AUCs of 0.8 and $0.\overline{66}$ respectively.

Though not perfect *AUC* is a reasonable measure of goodness of fit.

5.3.5. Positive Predictive Value (PPV)

Positive Predictive Value (*PPV*) is how likely a positive classification is to be a true positive.

$$PPV = \frac{TruePositive}{TruePositive + FalsePositive} \tag{5-9}$$

We should note that Positive Predictive Value (*PPV*) is not dependent on *AUC*. It is possible to have a high *AUC* and a low *PPV*, or a low *AUC* and high *PPV*.

Our statistical models assign to every sample a probability (p) of being positive (e.g. positive NPV). Before we can calculate the *PPV* we must decide upon a threshold (T), above which we classify the sample as positive, and below which we classify it as negative. Once we have done this for every single sample in our dataset we can calculate the *PPV*.

We can now repeat this procedure for any number of thresholds (T) in the range [0 , 1]. Let us illustrate the process with a flowchart:

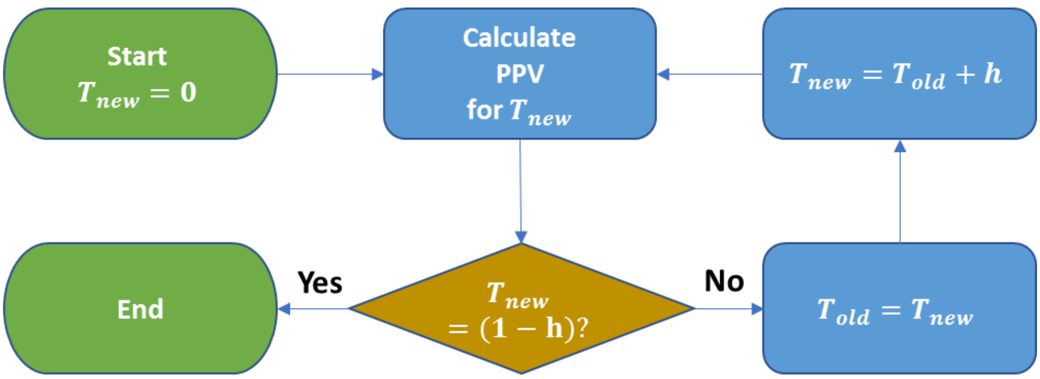

Figure 5-4:Flowchart for PPV calculations for PPV chart. Here h is a very small number.

If *h* was an infinitesimal we would now have an infinite number NPVs. If we were to place them on a scatterplot they would then form a line. If we merely calculate a large number of points and link them up we shall, however, reach a good approximation of this line.

Figure 5-5 below shows a set of sample *PPV* curves which illustrate the principle.

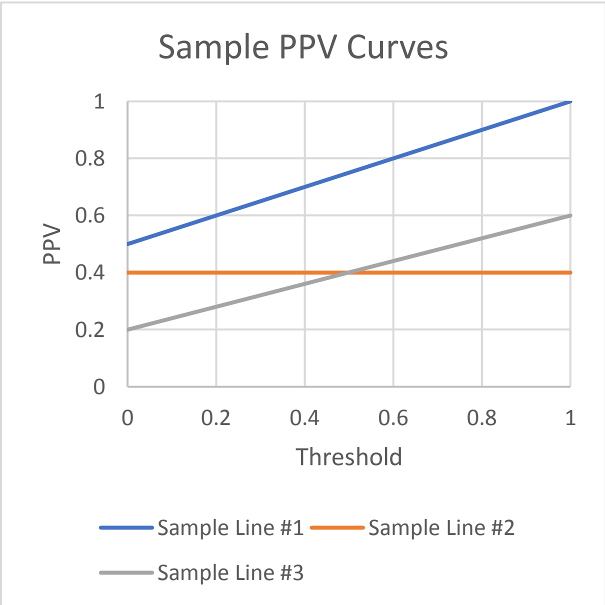

Figure 5-5: Sample PPV curves

As we can see Sample Line #2 has a superior PPV over Sample Line #3 until Threshold 0.5, after which Sample Line #3 becomes superior. All the while Sample Line #1 is superior to #2 and #3 for all Threshold levels.

The ideal situation is one where one single curve (like Sample Line #1 here) is superior to all others regardless of threshold.

6. Results and Discussion

6.1. Verification of Our Model

Given the importance of our model for our thesis it needs to be relevant, traceable, and tractable. Since we are mostly interested in the NPV and the factors that influence it we can say that our model is *relevant*. That is given inputs within the ranges discussed in section 4.5. our model will provide expected NPVs (either as magnitudes or as probabilities of a positive NPV). It is *traceable*, in that we spent section 4. Theory, Structure & Assumptions explaining the logic behind our assumptions and variables, and how they come together. Finally, it is *tractable*, we were able to program a simulation of the model and run it on the computer hardware available to us.

There is a popular saying that "all models are wrong, but some are useful." We believe that our model is useful for calculating expected NPV, and the probability of a positive NPV. The model has a sensible structure, and we can update the ranges it uses for its variables as needed.

However, it would be good to compare the result of our model to those of other models. In particular we could compare $P_{onshore}$ (the price of ammonia necessary for $NPV_{onshore} = 0$) to estimates made by other parties. We found a few sources, such as the one by the Royal Society (2020) which makes an estimate of projected green ammonia prices given some base assumptions. However the article by Nayak-Luke and Bañares-Alcántara (2020), appears more relevant for us. This article goes into some details on the LCOA (Levelized Cost Of Ammonia) for an islanded production plant that uses only green energy.

In their article they define the LCOA as:

$$LCOA = \frac{\sum_{t=0}^{T} \frac{CAPEX_t + OPEX_t}{(1+r)^t}}{\sum_{t=0}^{T} \frac{m_{NH_3}}{(1+r)^t}} \tag{6-1}$$

Here m_{NH_3} is the mass of ammonia produced in each given segment of time.

This is not the same method for calculating $P_{onshore}$ as found in section 4.1. , but it does appear to be a similar process.

Nayak-Luke and Bañares-Alcántara (2020) are investigating a set of specific sites, using a genetic algorithm to optimize certain variables for a minimal LCOA at that site. They are also using both wind and solar energy, thus potentially allowing for a more effective allocation of resources, compared to our approach. This is made even more effective by the fact that they have not taken our approach of treating the power supply as something that needs to be steady 24/7. Rather their approach is to overproduce hydrogen (the most energy demanding part of the process), thus building up a stockpile, which is then slowly fed into the ammonia plant itself. This approach is likely better at coping with fluctuations in the power supply, since they can stop producing hydrogen while still making ammonia from stockpiled hydrogen.

Their specific LCOA estimates are given in dollars, and converting to Euros (according to the exchange rate in June 2020, the time the article was written) we get a range LCOA for a multi-national corporation of €421-€2193 with a median of €856, while the LCOA for a domestic corporation goes from €433-€2656 with a median of €941.

Let us now produce a PDF curve for $P_{onshore}$ and mark in the 0.025 mark, the mode, the 0.5 mark, the 0.975 mark, and the two median values from Nayak-Luke and Bañares-Alcántara (2020).

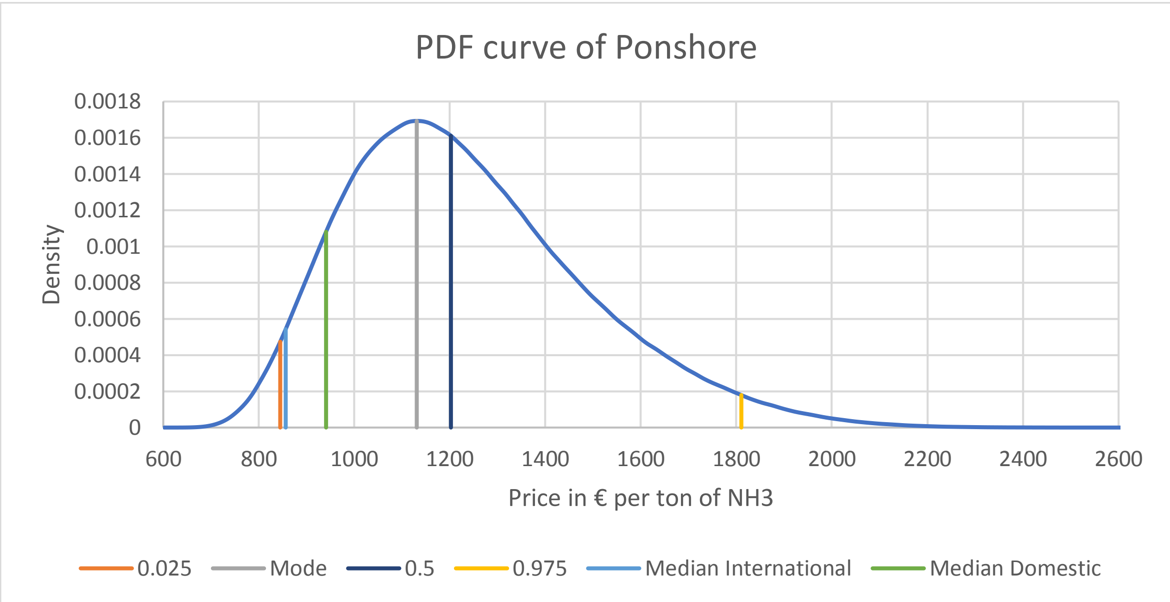

Figure 6-1: PDF curve of $P_{onshore}$ with key values marked.

The values from Nayak-Luke and Bañares-Alcántara (2020) have roughly the same range as ours. However, they have both a lower minimum and median. Their medians do however reside within our 0.95 confidence interval. This in spite of their very different approach, since we used a simple Monte Carlo simulation and have not made any attempts at minimizing $P_{onshore}$.

All the same the fact that we are reaching roughly the same ballpark figures as other researchers is encouraging. We will discuss these prices further in section 6.8. Further Discussions of the Price of Ammonia.

6.2. Sensitivity Tests of NPV

As we mentioned in section 5.2. we carried out our sensitivity analysis by setting each independent variable (see Table 4-3) in turn to its high, low and medium (halfway between high and low) values, while keeping the values of the other independent variables at medium.

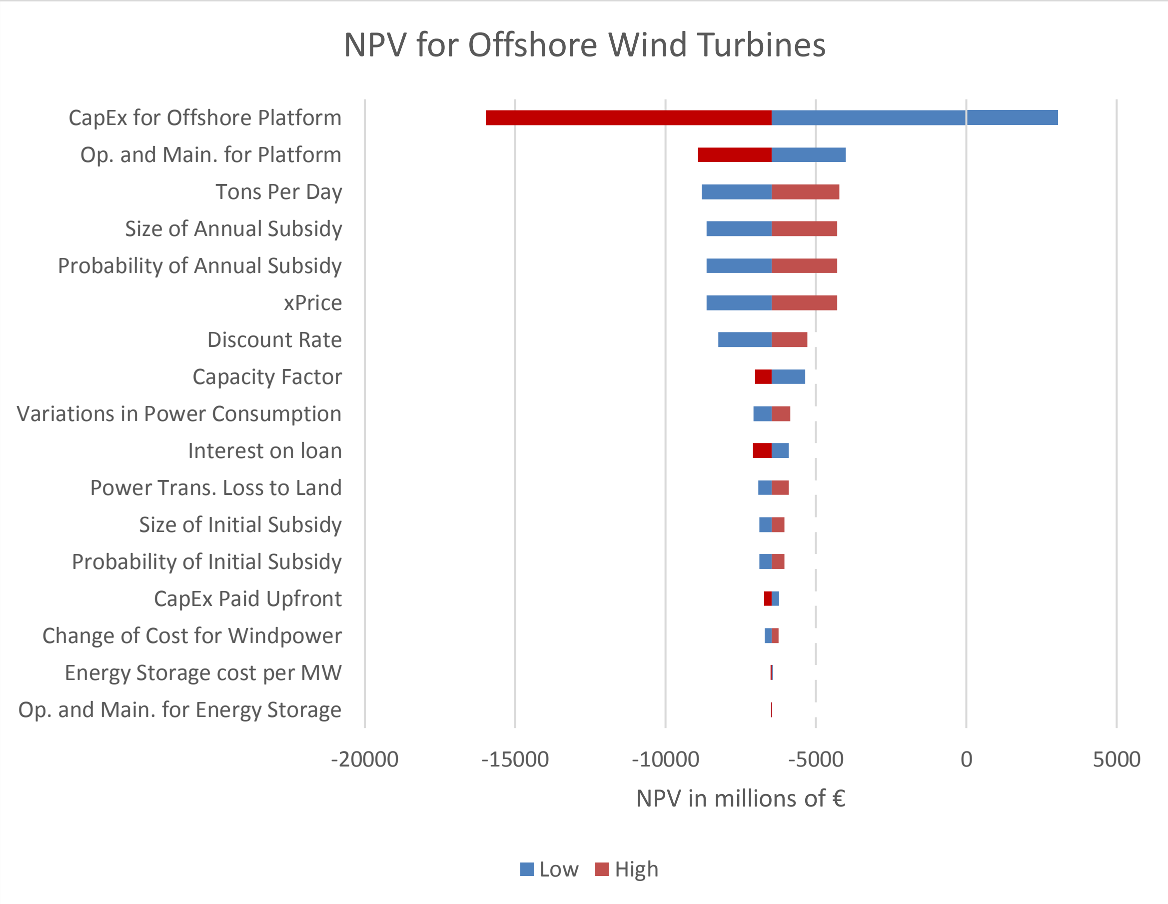

Figure 6-2: Sensitivity test of NPV for Offshore Windturbines

As we can see in the sensitivity tests for both offshore wind turbines and geothermal power the CapEx of the offshore platform dominates. It is the only factor which on its own can cross the boundary from negative to positive NPV. Not only that, but the operations and maintenance rate of the offshore platform is in the top three factors, along with tons per day (that is production per day).

One somewhat unexpected point is that “Change of Cost for Wind Power” affects the NPV for geothermal power.

This, however, becomes explicable when you look at sections 4.1. and 4.6.8. , we know that the price $p_{actual} = p_{onshore} \times xPrice$ (where p_{actual} is the actual market price of offshore green ammonia (OGA), while $p_{onshore}$ is the market price of onshore green ammonia). If $p_{onshore}$ is set so that $NPV_{onshore} = 0$, then anything that significantly affects the cashflows of the onshore green ammonia plant (such as CCWind or "Change of Cost for Wind Power") will also affect the NPV of the geothermal energy project.

This effect is in other words a result of assumptions made in our model.

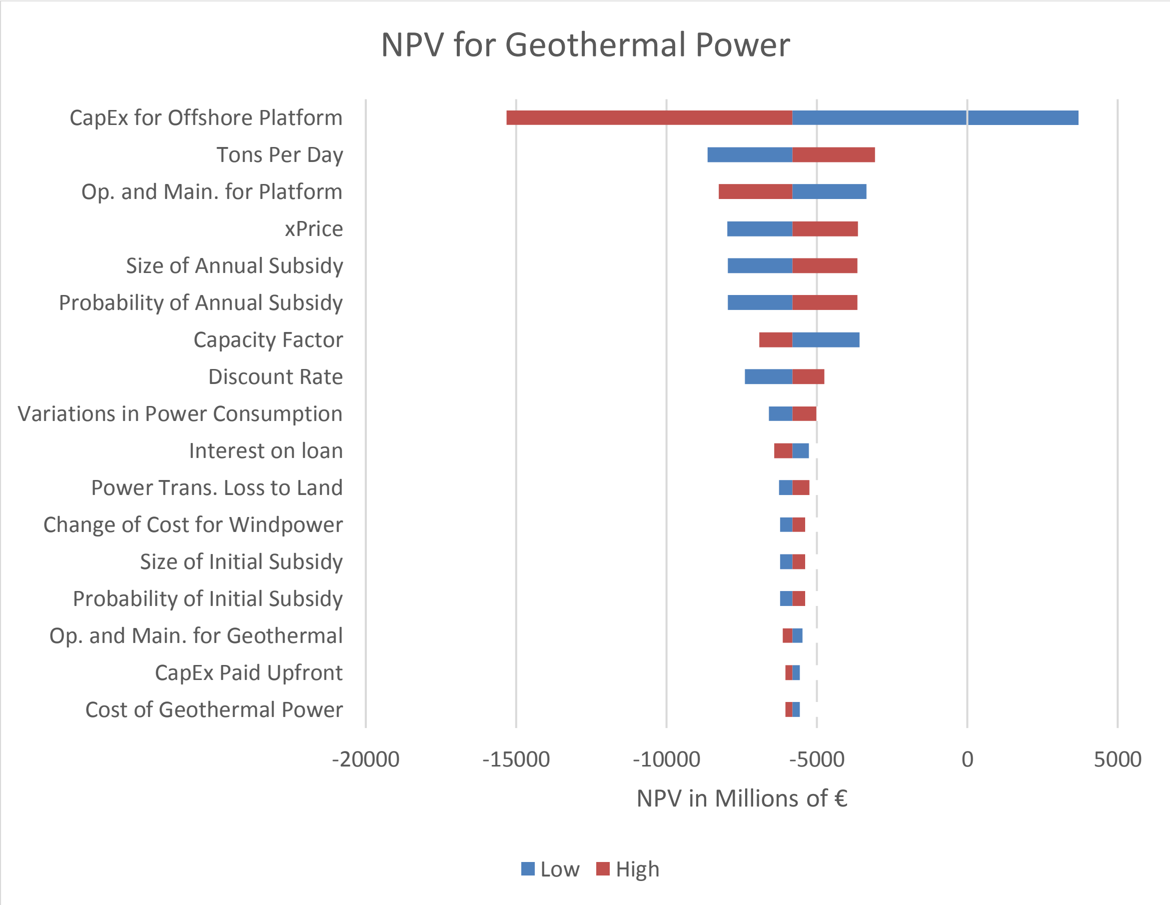

Figure 6-3:Sensitivity test of NPV for Geothermal Power

6.3. Relationship Between Key Variables and the Magnitude of NPV

From the sensitivity graphs above we see that there appears to be a strong link between NPV and both TonsPrDay (tons of ammonia produced a day) and CapExPlatform (capital expense for offshore platform). Let us here also include annual operations and maintenance costs (OpNMainPlatform) such that:

$$x_1 = \text{Tons per day} \tag{6-2}$$

$$x_2 = \text{CapExPlatform in millions} \tag{6-3}$$

$$x_3 = \text{OpNMainPlatform} \tag{6-4}$$

Looking at statistical models to explain that we found a model of the type:

$$NPV = \beta_0 + \beta_{11}x_1 + \beta_{21}x_2 + \beta_{22}x_2^2 + \epsilon \tag{6-5}$$

Gives an $R^2 > 0.64$ for both offshore windturbines and geothermal power.

It should be noted that a model of the type:

$$NPV = \beta_0 + \beta_{11}x_1 + \beta_{21}x_2 + \beta_{22}x_2^2 + \beta_{31}x_3 + \epsilon \tag{6-6}$$

Gives an $R^2 > 0.68$ for both offshore windturbines and geothermal power.

We ran tests on these models as both straight linear models and as generalized linear models, giving us both R^2 and AIC, providing us with the following table of coefficients:

	Offshore Wind Turbine		**Geothermal Power**	
	2-Predictors	**3-Predictors**	**2-Predictors**	**3-Predictors**
β_0	5.026e+07	3.789e+09	4.469e+07	3.788e+09
β_{11}	-7.651e+05	-7.650e+05	-7.644e+05	-7.643e+05
β_{21}	2.911e+06	2.919e+06	3.574e+06	3.581e+06
β_{22}	-6.248e+01	-6.555e+01	-5.666e+01	-5.974e+01
β_{31}	0	-1.248e+11	0	-1.250e+11
R^2	0.6422	0.6833	0.6408	0.6807
AIC	94359521	94115505	94433088	94197753
ΔAIC		-244016		-235335

Table 6-1: NPV Coefficients

We can see that the three predictor models are superior both in terms of R^2 and ΔAIC. However, the two predictor models open for presenting our findings in easy to grasp graphical formats.

6.4. Relationship Between TonsPrDay, CapExPlatform, and Positive or Negative NPV

As we mentioned briefly in section 5.3. it is often convenient to treat NPV as a binary variable: positive or negative. To demonstrate this let us make a scatterplot (Figure 6-4 below) in which positive NPVs are in blue and negative NPVs are in red, we immediately see a pattern:

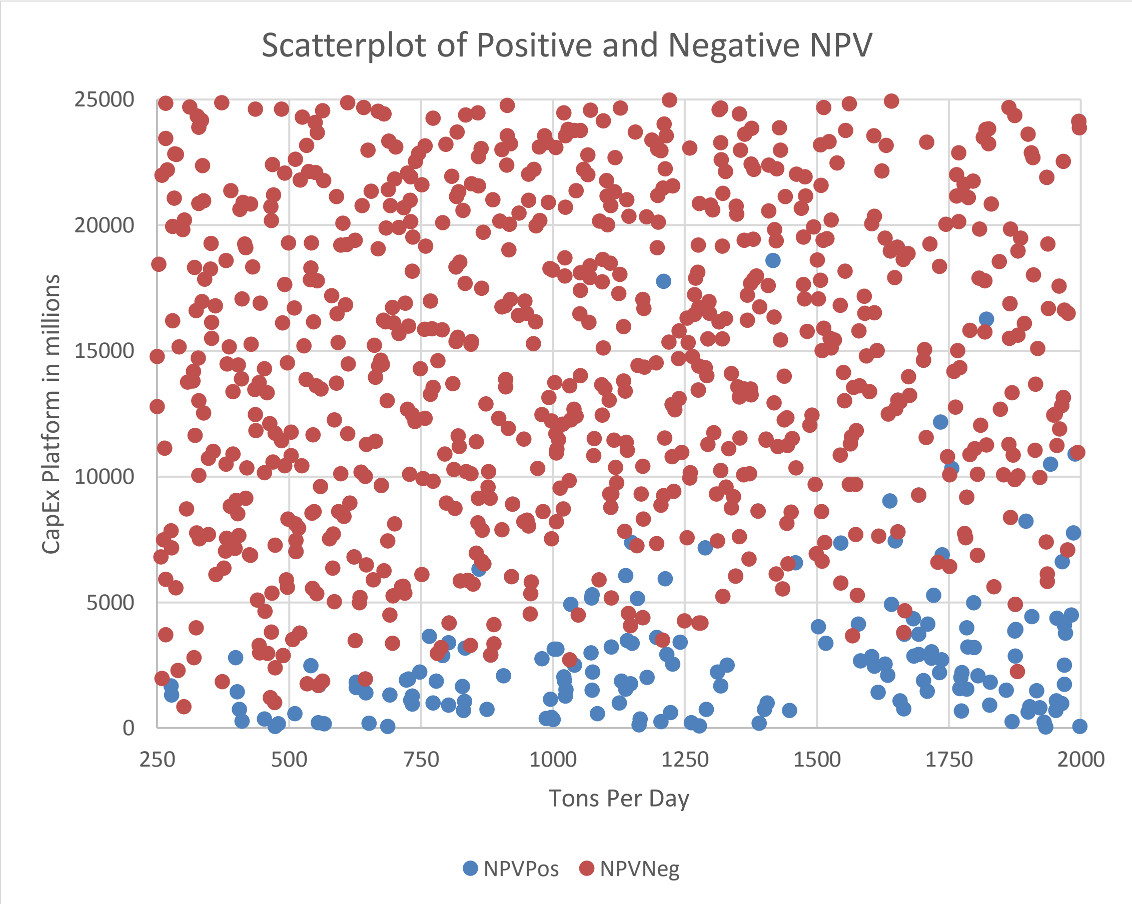

Figure 6-4: Scatterplot of Positive and Negative NPV

Since we are only looking at two possibilities here (NPVPos or NPVNeg) we have a binary response variable. This means that we can use a Bernoulli distribution to find the probability of a successful experiment (positive NPV) given various values of TonsPrDay and CapExPlatform.

$$x_1 = \text{Tons per day} \tag{6-7}$$

$$x_2 = CapExPlatform \tag{6-8}$$

It would be useful to note that, as shown in section 4.6.7. there is the possibility of subsidies affecting capital expenses. In our model subsidies are treated as removing some proportion of the capital expenses.

So, in terms of NPV calculation the modified CapEx (x_2) for the platform could be approximated by:

$$x_2 = CapExPlatform(1 - SubProp) \tag{6-9}$$

Where:

$$SubProp = SubInitProp \times CapExUpfront + SubAnnProp \times (1 - CapExUpfront) \tag{6-10}$$

A good many of the outliers of blue (NPVpos) dots in Figure 6-4 are due to the fact that a very high unmodified CapEx may have a very low modified counterpart due to high subsidies.

So which CapExPlatform should we be looking at? Modified or unmodified? We decided to investigate both.

We also wanted to see what would happen if we had a dataset which had no subsidies in the first place. Let us call this new dataset the NS dataset, where $SubInitProp = SubAnnProp = 0$ for all samples.

Name	Abbr.	X_2 formula	Source
Unmodified CapEx	UMC	$CapExPlatform$	Stand. train. dataset
Modified CapEx	MC	$CapExPlatform(1 - SubProp)$	Stand. train. dataset
CapEx (No Subsidies)	NS	$CapExPlatform$	NS training dataset

Table 6-2: Name and abbreviation for statistical models, as well as their x_2 formulas (how the x2 is calculated from CapExPlatform and SubProp), and the source of the data used to generate them.

And let us reiterate the meaning of the datasets:

Dataset Name	Size	Description
Standard training dataset	10^6	Generated by a Monte Carlo simulation according to the rules laid out in section 4 and with all variables having the ranges in Table 4-3. This is the dataset used to fit UMC and MC models.
NS training dataset	10^6	As above, but all $SubInitProp = SubAnnProp = 0$. This is the dataset used to fit the NS model.

Table 6-3: Training datasets

As mentioned in section 5.3. we used R to find the best model for our data. In this case for any given observation of x_1 and x_2 we are interested in finding the probability of getting a positive NPV, or formally $P(NPVpos|\boldsymbol{X})$ where $\boldsymbol{X} = [x_1, x_2]$. As mentioned in section 5.3.1. we used polynomial multivariable regression, with the possibility of uneven polynomials, for both x_1 and x_2. This was done separately for all six scenarios (UMC, MC, and NS for both wind power and geothermal power). In all cases the best result was found by an unequal multivariable polynomial where x_1 is in the 3rd or 4th degree and x_2 is in the 6th degree.

We should note that we did not test polynomials beyond the 6th degree, indeed experts consulted indicated that only the exceptionally high degree of samples (10^6) justified even this.

Thus, we get:

$$p = \frac{1}{1 + \exp(-\boldsymbol{x}'\boldsymbol{\beta})} \tag{6-11}$$

$$\begin{aligned}\boldsymbol{x}'\boldsymbol{\beta} = \beta_0 + \beta_{11}x_1 + \beta_{12}x_1^2 + \beta_{13}x_1^3 + \beta_{14}x_1^4 + \beta_{21}x_2 + \beta_{22}x_2^2 \\ + \beta_{23}x_2^3 + \beta_{24}x_2^4 + \beta_{25}x_2^5 + \beta_{26}x_2^6\end{aligned} \tag{6-12}$$

Here p can also be written as $P(NPVpos|\boldsymbol{X})$

Please note that in Table 6-4 (below) where β_{14} is set to zero that means that the model in question has x_1 in the 3rd degree (see section 5.3.1.). For reminders of what x_1 and x_2 stand for see eqn (6-7) for x_1 and Table 6-2 for x_2.

	Offshore Wind Turbine			Geothermal Power		
	UMC	**MC**	**NS**	**UMC**	**MC**	**NS**
β_0	5.483e-01	-3.902e-01	2.075e-01	3.871e-01	-3.425e-01	4.448e-01
β_{11}	6.895e-03	9.177e-03	7.172e-03	1.060e-02	8.908e-03	8.609e-03
β_{12}	-3.234e-06	-6.107e-06	-3.210e-06	-7.958e-06	-5.313e-06	-3.993e-06
β_{13}	6.311e-10	2.530e-09	6.514e-10	3.308e-09	2.006e-09	8.108e-10
β_{14}	0	-4.235e-13	0	-5.458e-13	-3.126e-13	0
β_{21}	-2.606e-03	-4.176e-03	-4.123e-03	-2.721e-03	-3.423e-03	-3.803e-03
β_{22}	5.074e-07	1.226e-06	1.226e-06	5.000e-07	8.108e-07	8.863e-07
β_{23}	-5.812e-11	-2.114e-10	-2.143e-10	-5.440e-11	-1.159e-10	-1.235e-10
β_{24}	3.610e-15	1.891e-14	1.929e-14	3.243e-15	8.813e-15	9.189e-15
β_{25}	-1.131e-19	-8.235e-19	-8.429e-19	-9.828e-20	-3.339e-19	-3.415e-19
β_{26}	1.395e-24	1.344e-23	1.379e-23	1.181e-24	4.893e-24	4.918e-24

Table 6-4: Coefficients for the probability of getting a positive NPV, covering offshore wind turbines and geothermal power, for CapEx of Platforms unmodified, modified with subsidies, and for a population where no subsidies are given. ***UMC****: Unmodified CapEx;* ***MC****: Modified CapEx, e.g. deducting subsidies;* ***NS****: No Subsidies, e.g. a dataset from a simulation run without subsidies.*

6.4.1. Explanation of NPV Probability Lines

For all six models and any given value of x_1 it can be shown mathematically (see appendix C) that p is strictly decreasing as x_2 increases, so as long as x_2 is in the range $[0\ , 22000]$. That means that the probability of getting a positive NPV is always decreasing the larger x_2 gets.

In the case of $x_2 > 22000$ there is a small chance that the probability function could behave poorly, but for all models this is where $P(NPVpos|\boldsymbol{X}) < 0.05$ and so we judge the issue to be of minimal importance (a decision maker is unlikely to be interested in projects with less than 5% chance of success).

This means that for any given value p_x such that $p_x \in [0.05\ , 1)$, where x_1 is given, there is always a unique value U of x_2 in the range $[0\ , 22000]$ such that $x_2|(p = p_x, x_1) = U$. Or to express it another way, for any value of $p_x \in [0.1\ , 1)$, and $x_1 \in [250\ , 2000]$, we can calculate all the corresponding, unique x_2 values.

If, for a given value p_x, and $x_1 \in [250\,, 2000]$, we plot each points $(x_1, x_2|(p = p_x, x_1))$, we would have an infinite number of points forming a line.

Let us call this a probability line. On this probability line the probability of a positive NPV is exactly p_x. Above the line $p < p_x$ because p is strictly decreasing as x_2 increases. Below the line $p > p_x$ because p is strictly increasing as x_2 decreases.

Of course, we cannot calculate an infinite number of points, but if we set $x_1 \in \{250{,}251, \dots ,2000\}$ (e.g. each integer from 250 to 2000) this gives us enough points to approximate our line. Let us make a separate probability line for $p_x \in \{0.1{,}0.2, \dots ,0.9\}$, each of them labelled 0.1,0.2,…,0.9.

Finally, we draw these lines over the previous scatterplot to give an illustration of what this would look like. Remember, probability p of positive NPV increases constantly as x_2 decreases:

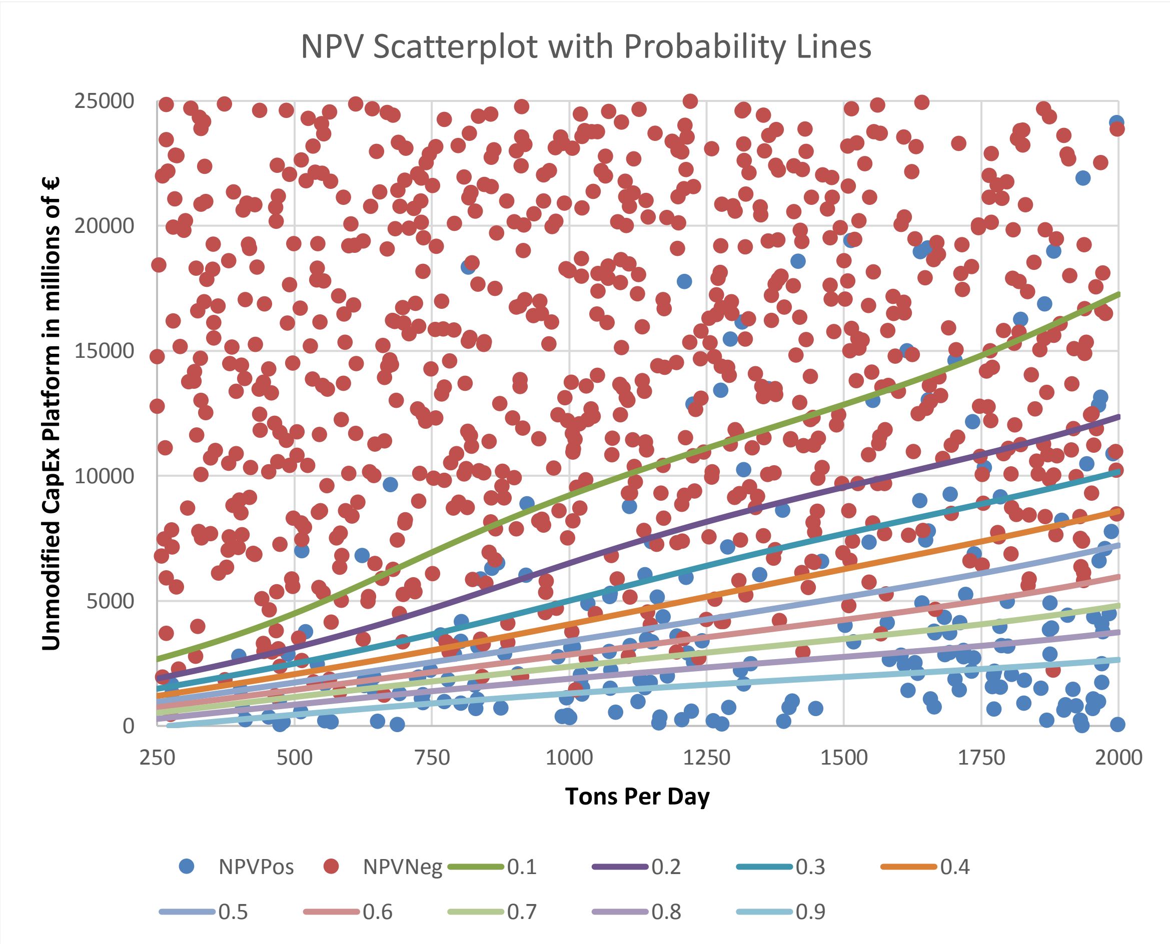

Figure 6-5: NPV scatterplot with Unmodified CapEx with Probability Lines projected over them

To give a quick example of how this specific chart could be used. If we have decided on a value, say 1500, for x_1 (Tons Per Day), we can move our finger up from that point and see that at about €1 950 million there is an 0.9 probability of a positive result. Further up we find that at €2750 million the probability has gone down to 0.8.

On the other hand, if we know that Tons Per Day is 1000 and CapEx is €5 000 million, we can quickly see that the probability of a positive NPV is 0.3.

Since we know that as x_2 (see Table 6-2) gets lower the probability always increases, we can do some extrapolation as well. For instance, at 1250 tons per day and €10 000 million we see that the point is somewhere between 0.1 and 0.2, a quick extrapolation is likely to get near the real number (0.13).

Note that these charts are meant for rule of thumb estimates, to be a quick decision aide. If precision is desired the exact probability can be calculated according to equations (6-11) and (6-12), combined with Table 6-4.

6.5. NPV Graphs with Unmodified CapEx, Modified CapEx, and No Subsidies

6.5.1. Offshore Wind Power

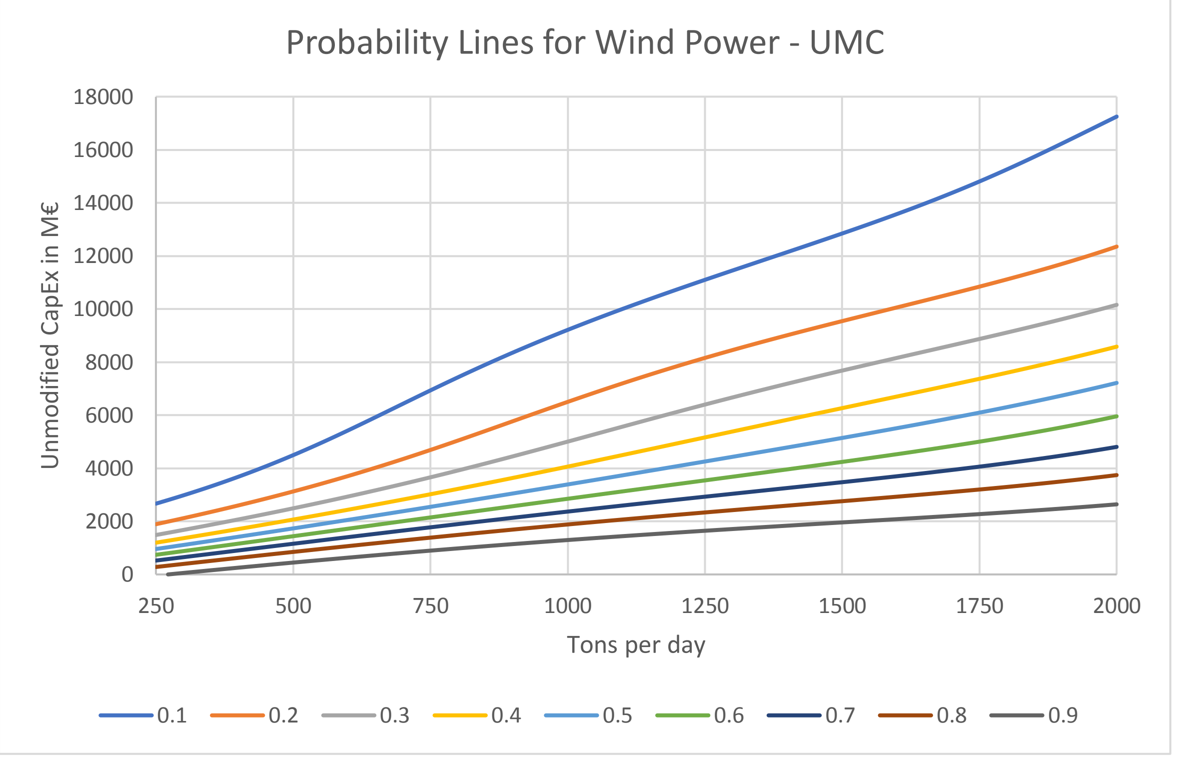

Figure 6-6: Probability of NPVPos for offshore wind power for UMC

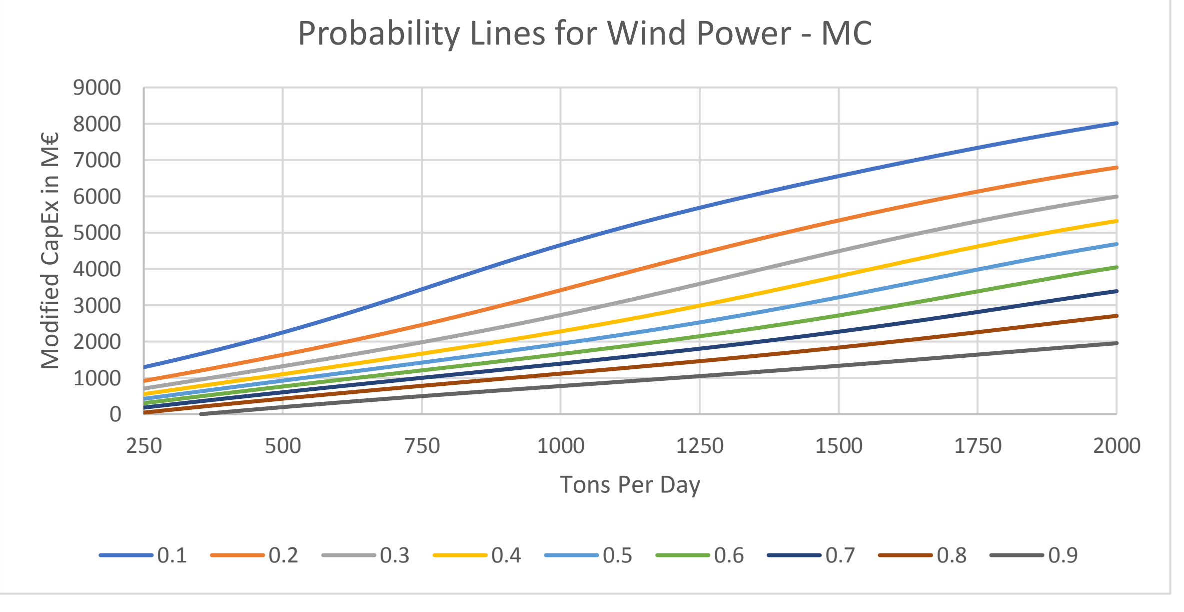

Figure 6-7: Probability of NPVPos for offshore wind power for MC

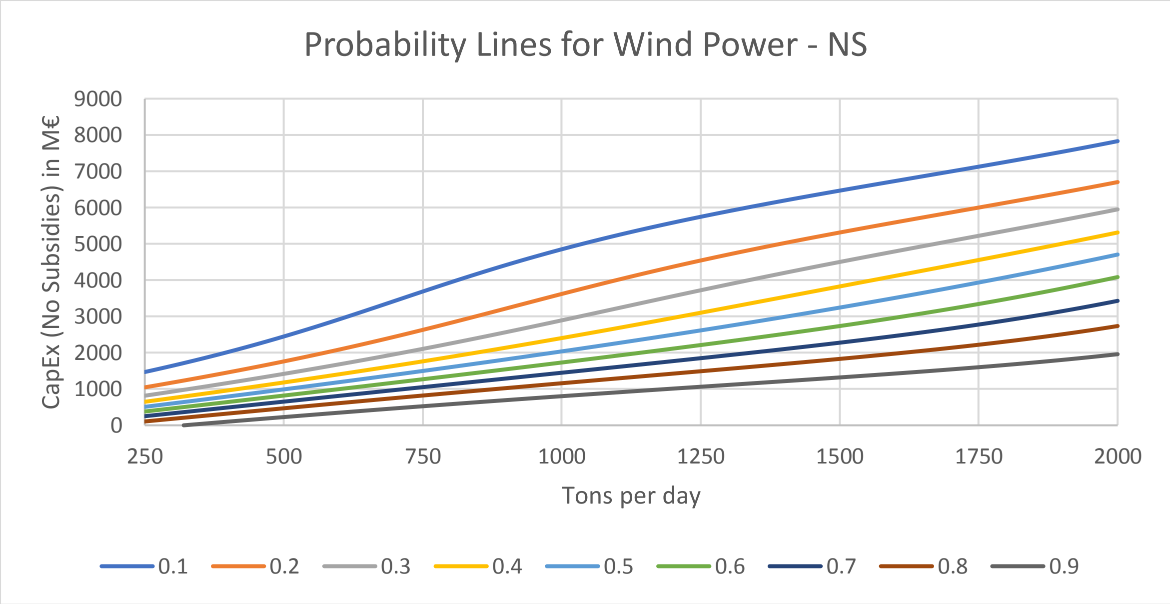

Figure 6-8: Probability of NPVPos for offshore wind power for a population sample where no subsidies were granted, e.g. NS.

6.5.2. Offshore Geothermal Power

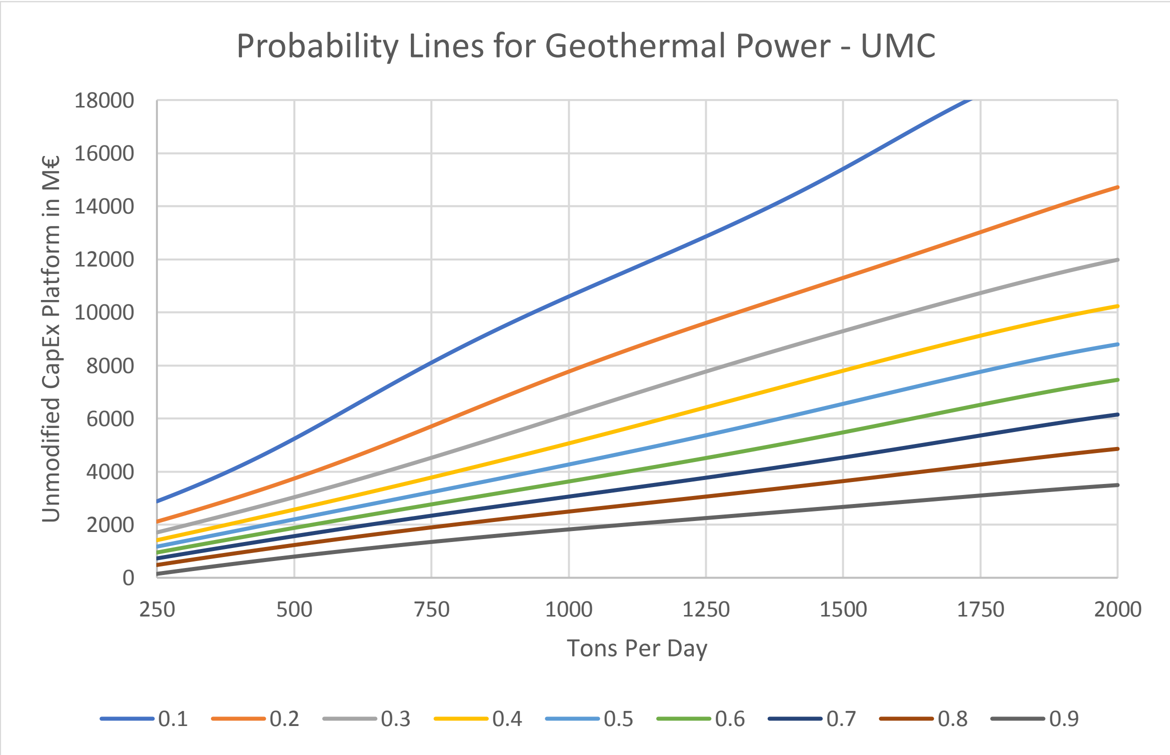

Figure 6-9:Probability of NPVPos for geothermal power for UMC

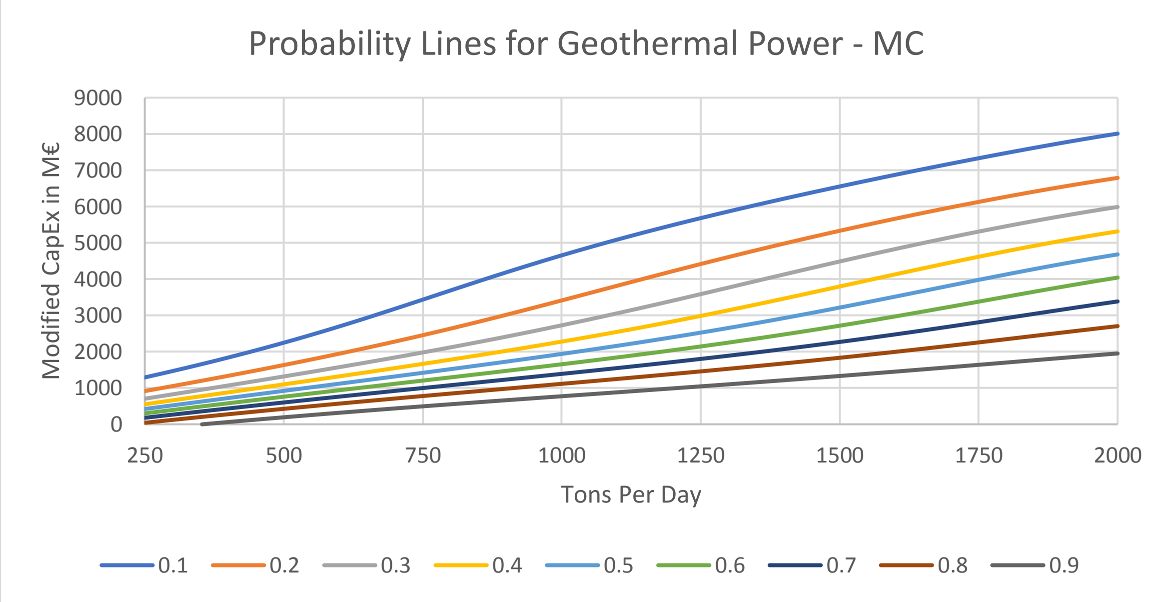

Figure 6-10:Probability of NPVPos for geothermal power for MC

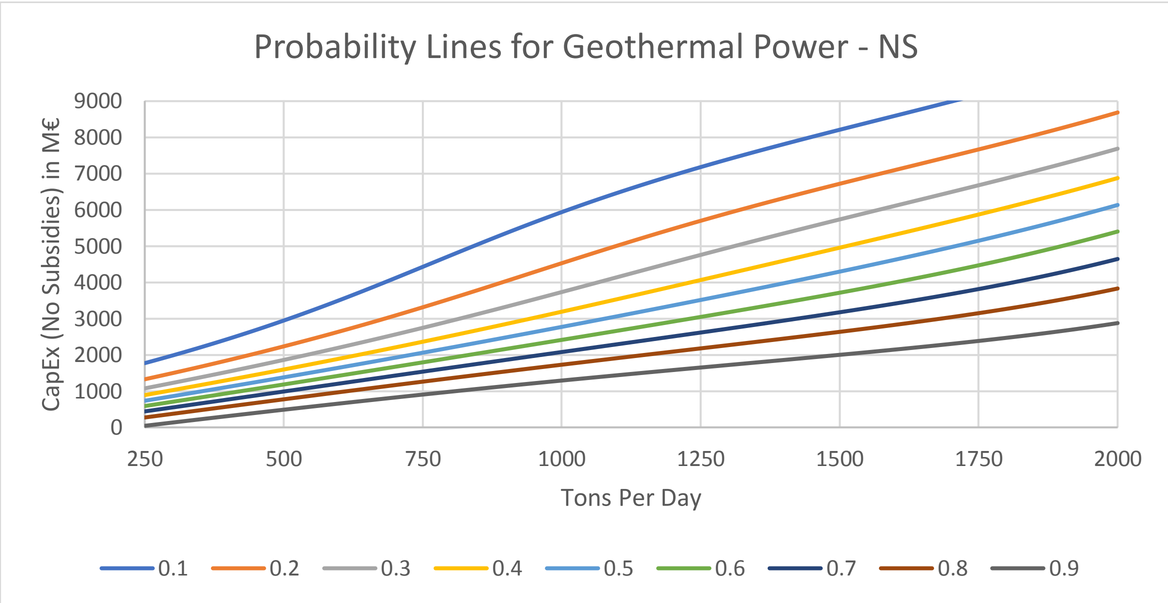

Figure 6-11: Probability of NPVPos for geothermal power for a population with no subsidies (NS)

6.6. Comparing Probability Lines

Looking at the probability lines of both wind power and geothermal power, we see that the ones for the respective MC model are very similar to those for the NS model. Let us compare the probability lines for wind power, we plot the probability lines in Figure 6-7 and Figure 6-8 (both above) into Figure 6-12 for probabilities of positive NPV being 0.1, 0.5, and 0.9. For completeness we also include the lines for UMC (Figure 6-6).

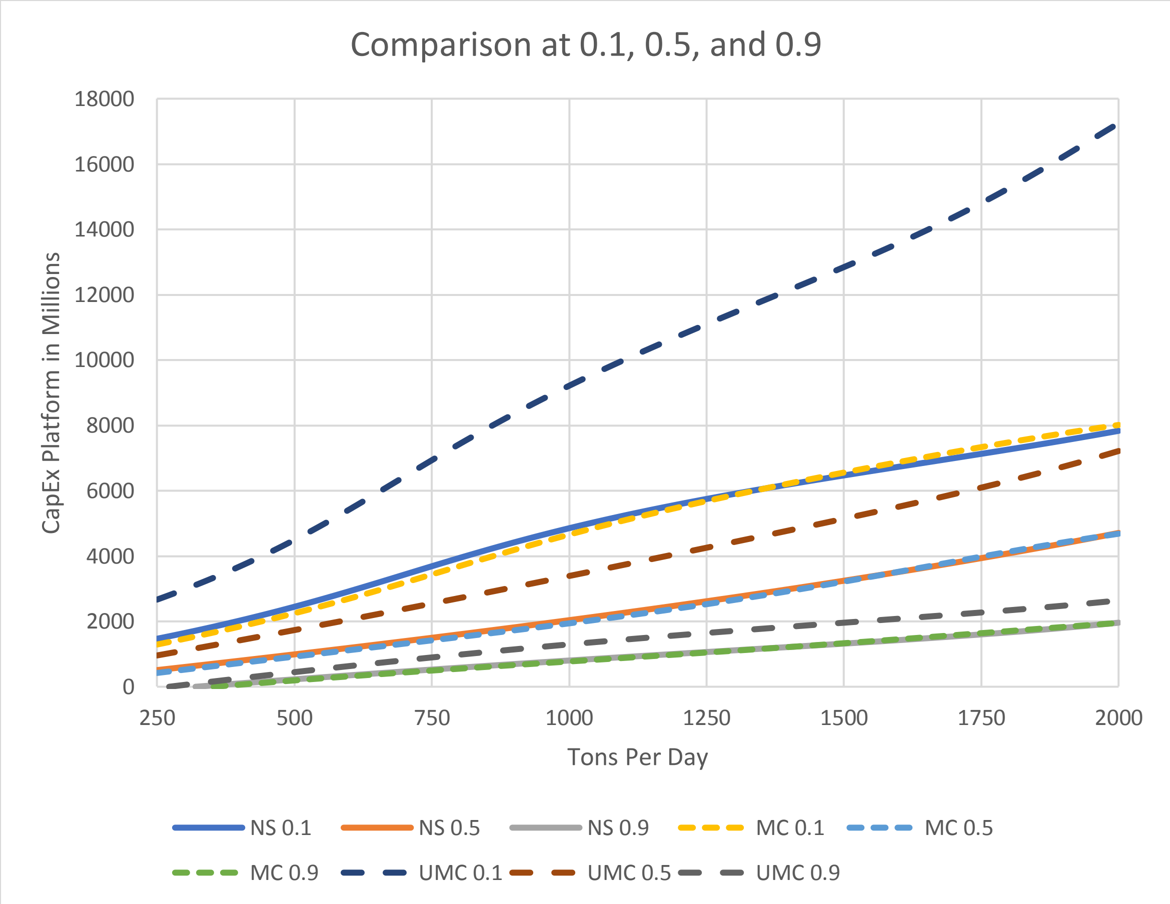

Figure 6-12: Comparative probability lines between NS (No Subsidies), MC (Modified CapEx) and UMC (Unmodified CapEx).

Although the lines for the NS and MC cases are very similar, they are not identical. Likewise, the parameters for the models used to generate them (see Table 6-4) also appear similar, but not identical.

At the moment, we have six different probability line charts: Wind-MC, Wind-NS, Wind-UMC, Geothermal-MC, Geothermal-NS, and Geothermal-UMC. Ideally, we would like to reduce this to a single chart. However, even a cursory investigation shows that wind and geothermal statistical models are so different that they cannot be effectively unified.

If we could retain only one graph for each of wind and geothermal energy, that would be very convenient. For quick rule of thumb estimates having a single chart to consult would be better than having to choose between three. Likewise, being able to present a single, simple to understand chart would make it easier to explain the issues to other stakeholders.

To see if this is something that is feasible, we could test each statistical model against the dataset and x_2 (see Table 6-2) used to generate the other models. We will go into this in the next section.

6.7. Testing and Comparing Goodness of Fit

Before we can give preference to any of our statistical models (UMC, MC, NS, etc) we must examine their goodness of fit. That is how well these models do against a test dataset. Since the probability lines are generated by way of the statistical models, they are as good or bad the models themselves.

During our tests we will be using two test datasets, as described below:

Dataset Name	Size	Description
Standard test dataset	10^6	Generated by a Monte Carlo simulation according to the rules laid out in section 4 and with all variables having the ranges in Table 4-3. This dataset is generated by the same rules used to fit UMC and MC.
NS test dataset	10^6	As above, but all $SubInitProp = SubAnnProp = 0$. This dataset is generated by the same rules used to fit NS.

Table 6-5: Test dataset

We will be testing our statistical models against these datasets, first against their regular test datasets, then we shall do a "cross" test datasets where we swap dataset and/or x_2 formula.

Testing models against Regular Datasets and X_2 (Self Test)			
Suffix	**Abbr.**	**X_2 formula**	**Source**
Geo or Wind	UMC##	$CapExPlatform$	Stand. test dataset
	MC##	$CapExPlatform(1 - SubProp)$	Stand. test dataset
	NS##	$CapExPlatform$	NS test dataset

Table 6-6: Testing statistical models against Regular Datasets and x_2. ## stands for the number of polynomials used for x_1 and x_2 respectively. x_2 formula is how the x2 is calculated from CapExPlatform and SubProp.

Testing models against Cross Dataset and X_2 (Cross Test)			
Suffix	**Abbr.**	**X_2 formula**	**Source**
Geo or Wind	UMC##MC	$CapExPlatform(1 - SubProp)$	Stand. test dataset
	UMC##NS	$CapExPlatform$	NS test dataset
	MC##NS	$CapExPlatform$	NS test dataset
	NS##MC	$CapExPlatform(1 - SubProp)$	Stand. test dataset

Table 6-7: Testing statistical models against Cross Datasets and x_2. ## stands for the number of polynomials used for x_1 and x_2 respectively.First set of letters is the model used, second is what it is crosstested against. x_2 formula is how the x2 is calculated from CapExPlatform and SubProp.

Note that these statistical models are the same ones as in the Self Test, the reason we add an MC or NS at the end of the abbreviation is to remind ourselves that this is a Cross Test and what dataset and $x_2$formula we were testing against.

In the rest of this chapter, unless otherwise specified, the term model will refer to these statistical models.

Since we in this case are dealing with a binary case, one obvious method of testing our data is to compare compare the Area Under the Curve for the Receiver Operating Characteristics, or the *AUC-ROC* as it is more generally called. *ROC* curves are a plot of the true positive rate (*TPR*) against the false positive rate (*FPR*), then we find the area under the curve (*AUC*) for more details on *AUC-ROC*, *TPR* and *FPR* see section 5.3.4.

Our *ROC* for Self Test (see Table 6-6) and Cross Test (see Table 6-7) are shown in Figure 6-13 and Figure 6-14 below:

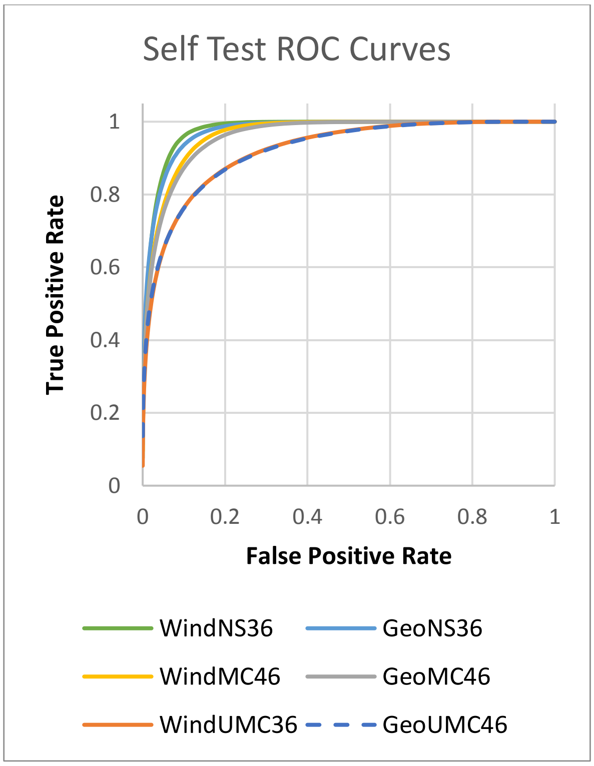

Figure 6-13: ROC chart of fits tested against their standard datasets and x_2 formulas (Self Test).See Table 6-6 for details.

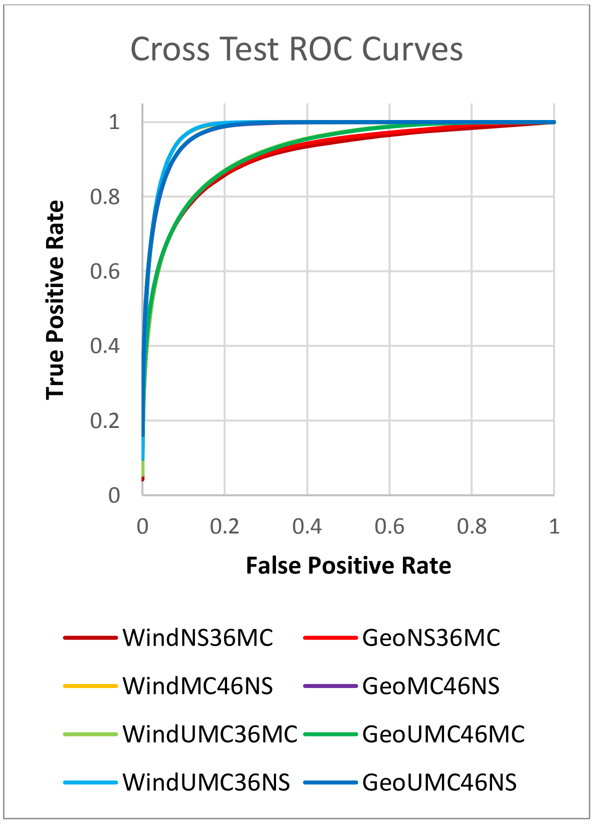

Figure 6-14: ROC chart of fits tested against cross datasets and x_2 formula. See Table 6-7 for details. Regrettably WindUMC36NS and GeoUMC46NS overlap with WindMC46NS and GeoMC46NS; Likewise WindUMC36MC and GeoUMC46MC overlap with WindNS36MC and GeoNS36MC.

Figure 6-13 shows that when tested against the standard dataset and x_2 formulas (Self Test) the NS (No Subsidies) and MC (Modified CapEx) models do quite well, whereas the UMC (Unmodified CapEx) models do quite badly. Whereas looking at the cross dataset and x_2 formulas (Cross Test) (Figure 6-14) we see that all of the models seem to do quite well when tested against the NS test dataset.

The $AUC\left(\frac{AreaUnderCurve}{TotalArea}\right)$ is, as stated in section 5.3.4. a measure where the ideal case is AUC=1. However, as we stated earlier there are some issues with AUC which may make it less than ideal (see sections 5.3.4. and 5.3.5.).

The Brier Score (Brier, 1950) (also see section 5.3.3.), which is a strictly proper scoring rule should be a better test of our models. For a case with only two cases (in our case positive or negative NPV) the Brief scoring rule can be simplified to:

$$BS = \frac{1}{N}\sum_{i=1}^{N}(f_i - E_i)^2 \qquad (6\text{-}13)$$

Where BS denotes the Brier Score, f_i is the model's calculated probability of a positive NPV for sample *i* in the dataset. E_i is 1 for a positive NPV and 0 for a negative NPV. The lower the score is, the better the model fits the dataset. We can now do a comparison:

Self Test			**Cross Test**		
MODELS	AUC	BS	MODELS	AUC	BS
WindNS36	0.977	0.037	WindNS36MC	0.907	0.060
GeoNS36	0.974	0.044	GeoNS36MC	0.913	0.069
WindMC46	0.964	0.061	WindMC46NS	0.978	0.037
GeoMC46	0.960	0.069	GeoMC46NS	0.974	0.045
WindUMC36	0.921	0.092	WindUMC36MC	0.921	0.083
GeoUMC46	0.921	0.084	GeoUMC46MC	0.921	0.095
			WindUMC36NS	0.978	0.053
			GeoUMC46NS	0.974	0.061

Table 6-8: AUC and BS for Test Dataset and Cross Test Dataset. Remember that models in the Self Test and Cross Test are the same, but in the Cross Test an NS or MC term is added to the end of the model name in order to remind us what dataset and x_2 formula it is tested against (see Table 6-6 and Table 6-7)

For the *BS* the results of these tests are fairly intuitive, and roughly in line with what we would expect. We see that both on the Self Test and Cross Test the NS and MC models get better results than the UMC models (remember that for the Cross Test we should compare NS##MC to UMC##MC and MC##NS to UMC##NS). We also note that between the Self Test and the Cross Test the NS and MC models appear to have almost switched *BS*, which further indicates how similar these models are.

It is the *AUC* that makes this interesting: In the Cross Test NS models have a much lower *AUC* than the MC models, while the MC models have a slightly higher *AUC* than in the Self Test.

It is important to remember that *BS* tells us something about how good our models are at classifying two classes. However, a decision maker might be more interested in avoiding false positives than false negatives. This is doubly important when we consider that there is an overweight of negative NPVs in our datasets, which could skew our results.

If we want to get true positives and avoid false positives we must look at Positive Predictive Value (*PPV*).

$$PPV = \frac{True\ Positives}{True\ Positives + False\ Positives} \tag{6-14}$$

Of course our models calculates the probability of each sample having positive NPV, so we will plot the PPV across a threshold range [0 , 1], see section 5.3.5. for more details on PPV and thresholds. However, briefly, if the probability of a positive result (positive NPV) is above the threshold the sample is classified as positive. We then plot the PPV curves across the entire threshold range to see if there are any interesting patterns.

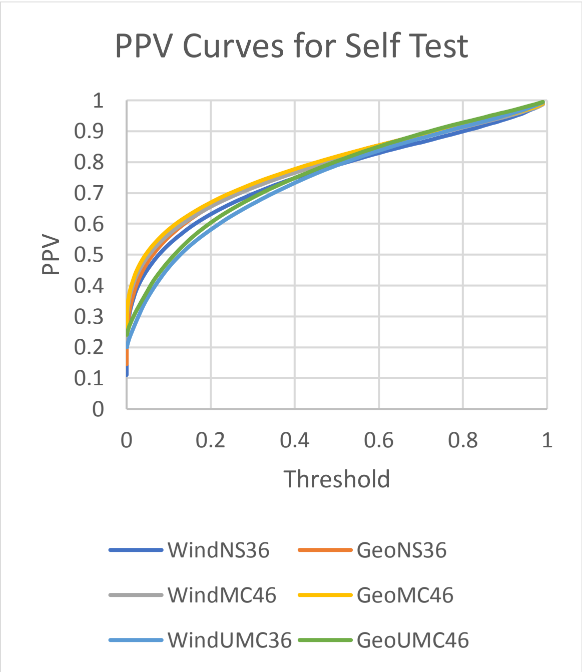

Figure 6-15: PPV curves for Self Test. See model description in Table 6-6

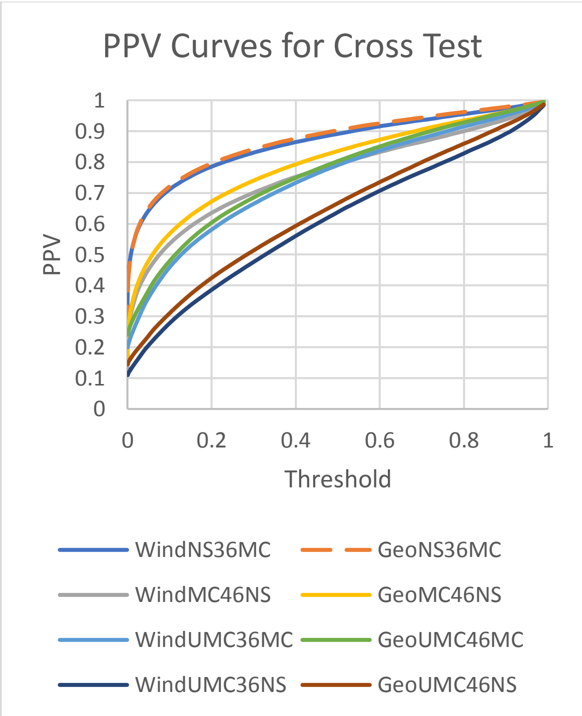

Figure 6-16: PPV curves for Cross Test. See model description in Table 6-7

What we can see is that the PPV curves are roughly the same for all models on the Self Test. However, on the Cross Test that changes: The NS models leap ahead and have superior PPV curves across the board.

Thus, two facts are established:

1. The *BS* of the NS model on the Cross Test was almost identical to the BS of the MC model on the Self Test.
2. The PPV of the NS model is superior to all other models on the Cross Test.

This argues that for preliminary analysis we can reject all other models in favour of the NS models, regardless of the x_2 formula used. This makes good sense since:

$$CapExPlatform(1 - SubProp) = CapExPlatform, \text{if } SubProp = 0 \tag{6-15}$$

And looking at the sensitivity chart in section 6.2. we can judge that the effect of *CapExPlatform* is so great that it overpowers the effect subsidies might have on other parts of *TotalCapitalExpense* (such as the cost of power generation or the ammonia plant itself).

So, using only the two NS models (for either wind power or geothermal power) the decision maker can, once they've decided on TonsPrDay, make a good estimate of the probability of positive NPV for any given x_2 ($CapExPlatform(1 - SubProp)$, being in mind *SubProp* can be zero). And the effect of any changes in *SubProp* (level of subsidies, see equation (6-10) on page 43) can also quickly be established.

6.8. Further Discussions of the Price of Ammonia

There are four prices we need to keep track of:

Price	Explanation
$P_{onshore}$	Break-even ammonia price that makes $NPV_{onshore} = 0$.
P_{actual}	Actual price the market will bear for offshore ammonia, $P_{actual} = xPrice \times P_{onshore}$
P_{wind}	Break-even ammonia price that makes $NPV_{wind} = 0$.
P_{geo}	Break-even ammonia price that makes $NPV_{geo} = 0$.

Table 6-9: Table of NH3 prices

In this work we have assumed that $NPV_{onshore} = 0$ and have set $P_{onshore}$ accordingly. So, by extension we have that:

$$\begin{aligned} P_* \leq P_{actual} &\Rightarrow NPV_* \geq 0 \\ P_* > P_{actual} &\Rightarrow NPV_* < 0 \end{aligned} \tag{6-16}$$

* stands for wind or geo. Should NPV be less than zero then the decision maker ought to reject that project.

6.8.1. PDF and CDF of the Prices (Onshore, Actual, Wind and Geothermal)

We will next examine the PDF and CDF of the prices:

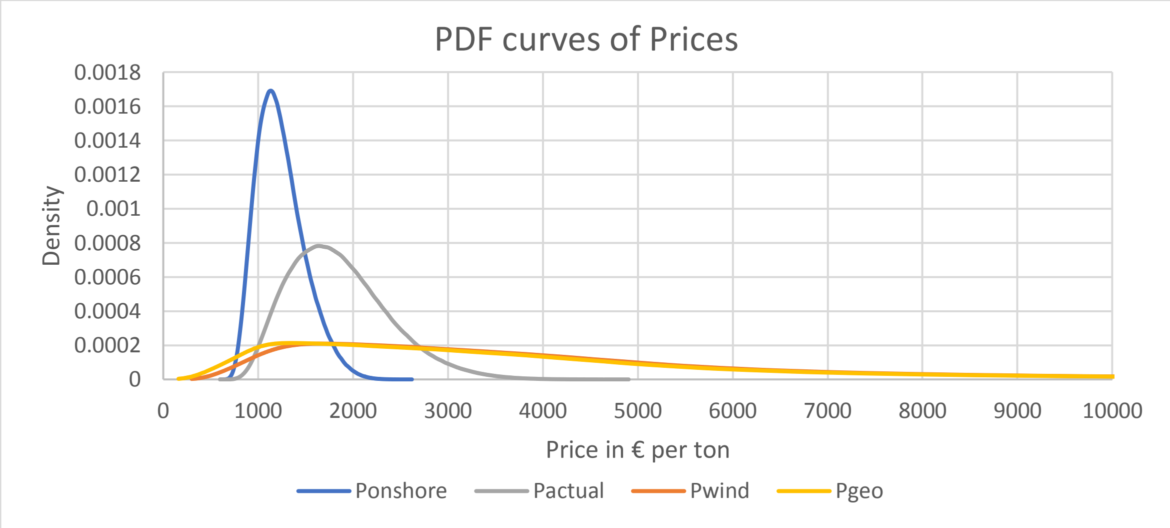

Figure 6-17: PDF curves of prices.

Figure 6-17 (above) shows that both P_{wind} and P_{geo} have very long tails to the right. We cut the figure at €10 000 per ton, but both P_{wind} and P_{geo} have tails stretching out to around €37 000 per ton. It is very unlikely that any green ammonia plant would be built, if it requires such extreme prices to be profitable.

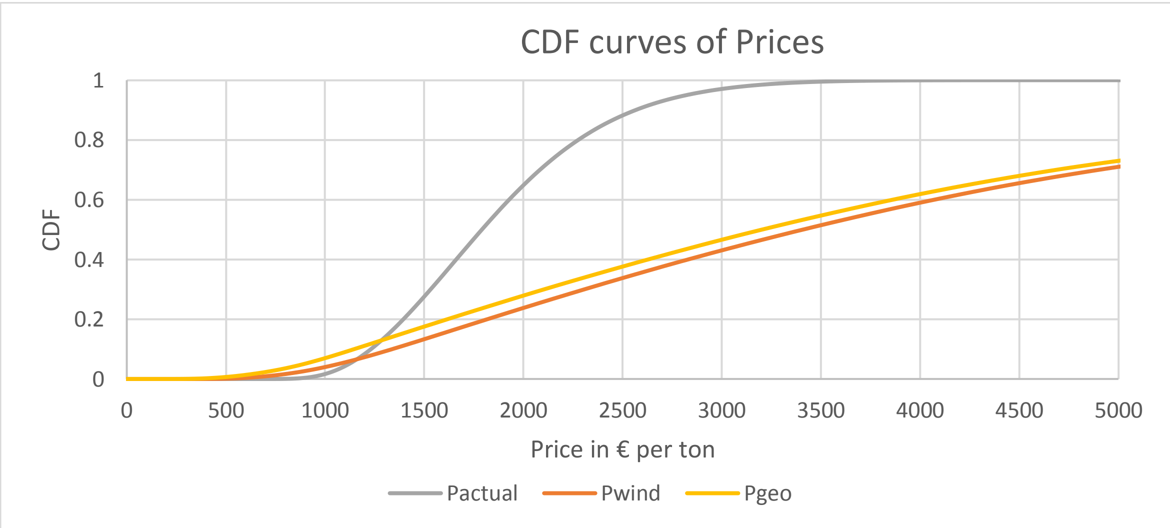

Figure 6-18: CDF curves of prices

From the CDF (Figure 6-18, above) we can see that it is possible, but somewhat unlikely that P_{wind} and P_{geo} will be low enough to permit a positive NPV.

However, the reason for these extreme values (and long PDF tails) likely correspond to Monte Carlo samples with an unlikely, and fairly extreme combination of factors. For further information on this see section 6.8.2. on sensitivity charts for prices.

6.8.2. Sensitivity Tests of Prices (Onshore, Actual, Wind and Geothermal)

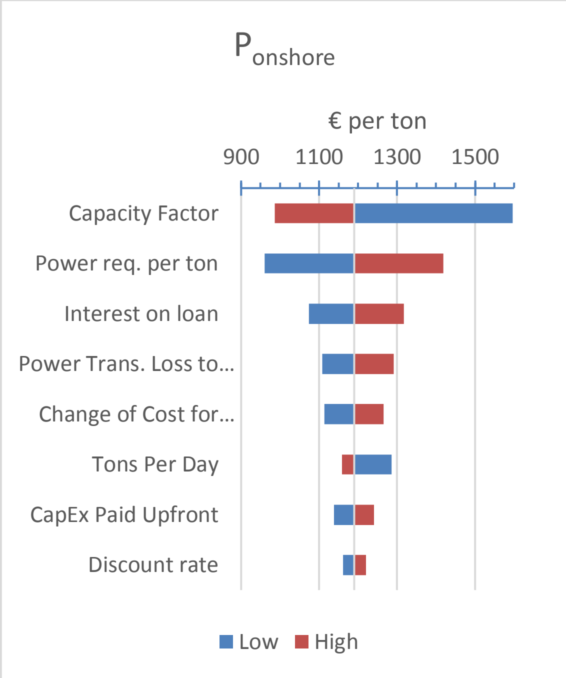

Figure 6-19: Sensitivity test for Ponshore

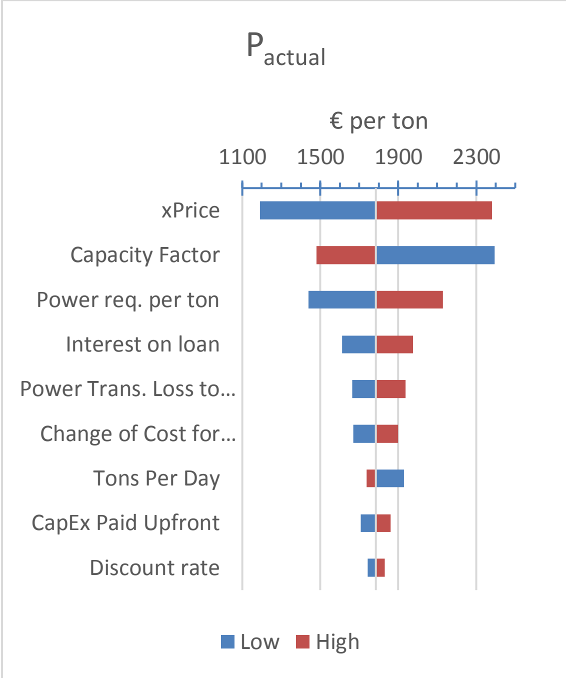

Figure 6-20: Sensitivity test for Pactual

As we can see there is fairly little in the way of extreme values. Overall, it appears that these sensitivity graphs (Figure 6-19 and Figure 6-20) can account for the variation that we see in Figure 6-17. Let us next look at sensitivity charts for P_{wind} and P_{geo}.

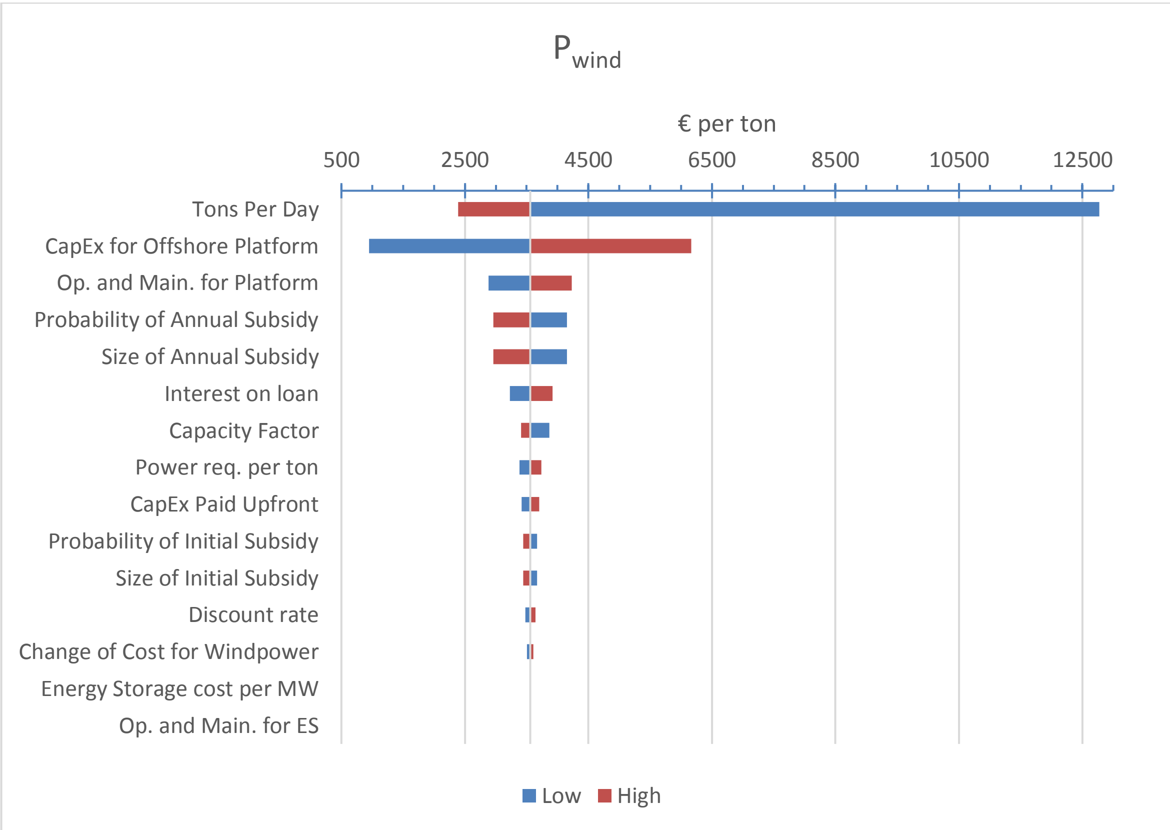

Figure 6-21:: Sensitivity test for Pwind

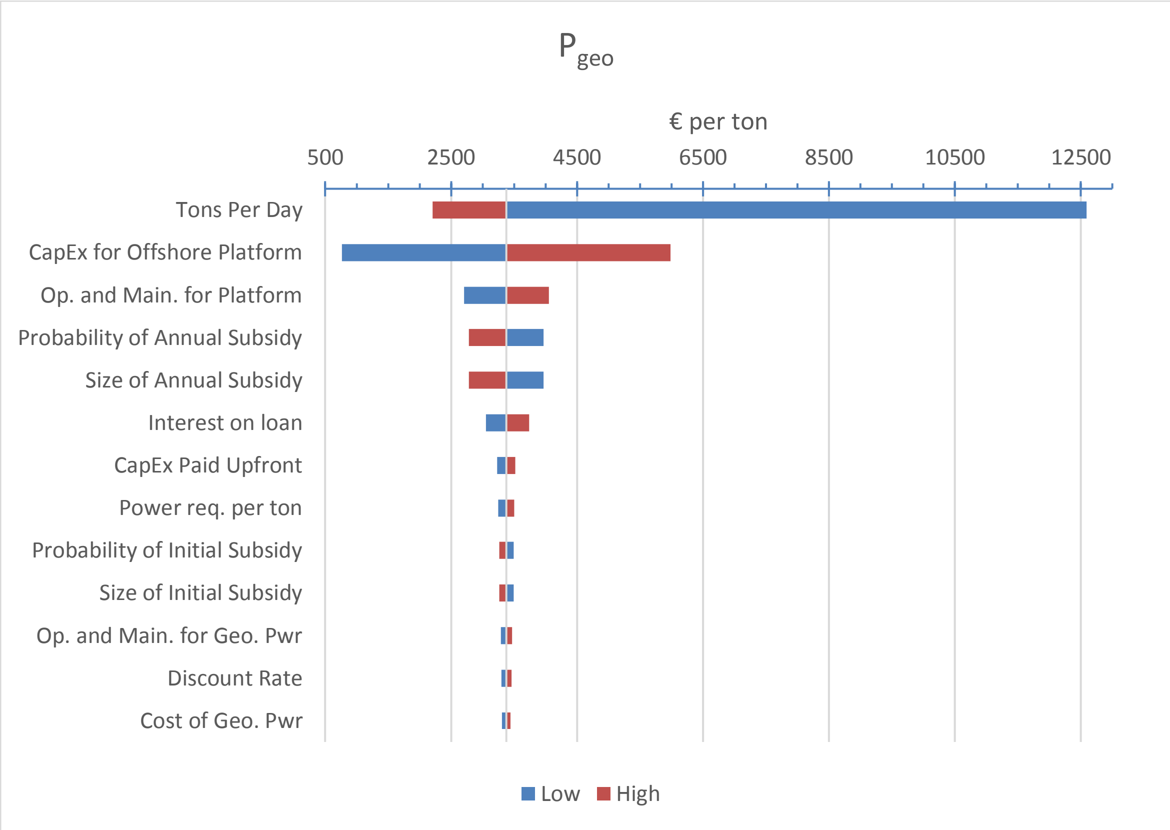

Figure 6-22: : Sensitivity test for Pgeo

As we would expect CapEx for the offshore platform has a great impact on both sensitivity charts. What is perhaps more surprising is that Tons Per Day has a greater impact. This becomes more explicable when we remember that the high and low variation of Tons Per Day is tested with a medium value for the CapEx of the offshore platform.

We therefore tested the combination of a high CapEx ($€25 \times 10^9$) with low Tons Per Day (250) and found that both P_{wind} and P_{geo} could easily reach €30 000 per ton.

These extreme potential prices confirm our need for a formula or model that can estimate CapEx for an offshore platform given the production capacity of the ammonia plant in Tons Per Day.

6.8.3. Comparing $P_{onshore}$ Against Other Price Estimates for Green Ammonia

In section 6.1. we point out that our estimated median and mode for $P_{onshore}$ is higher than the median estimate of Nayak-Luke and Bañares-Alcántara (2020). We discussed some possible reasons for this, mostly in terms of our assumptions and approach.

It will be illustrative to compare our estimates with actual or predicted ammonia prices. For instance, the maximum, mean and minimum spot prices of ammonia were €641, €379, and €147, respectively, for the period 2000-2019 (Nayak-Luke & Bañares-Alcántara, 2020)

These however are references for normal ammonia prices, but we are interested in the premium that might be paid on green ammonia. CF Industries[1] estimates a price of $2 200 (€1958) per ton of green ammonia (Tullo, 2021), which is the highest estimates we have seen so far. If the actual green ammonia price is the same as estimated by CF Industries (€1958/ton), there is a great chance that onshore green ammonia production will be profitable, but there is a fairly small chance that offshore green ammonia (powered by either wind or geothermal) will be profitable (given our assumptions and model).

We should note that once you get beyond a certain price threshold the probability of success (positive NPV) rapidly improves. In Table 6-10 (below) we include an estimate for prices of €1000 and €1250 per ton of ammonia, and we can see a very distinct effect on the probabilities.

Per ton of ammonia:		Probability of positive NPV for:		
Name of estimate	Price estimate	Onshore	Offshore Wind	Offshore Geo.
Min. spot price	€147	0	0	0
Mean spot price	€379	0	~0	0.002
Max. spot price	€641	~0	0.006	0.017
CF Ind. est.	€1958	0.992	0.229	0.271
Our low est.	€1000	0.173	0.070	0.040
Our high est.	€1250	0.574	0.122	0.083

Table 6-10: Probability of positive NPV given various estimated ammonia prices. ~0 is for very low estimates.

If these probabilities are accurate then any successful implementation of green ammonia might require either lower production costs (for instance by way of aggressive subsidies), and/or increasing the cost of other fuels by CO_2 taxes. The effects of CO_2 taxation is beyond the scope of this thesis.

[1] The CF in CF Industries is now a proper name, but it was originally an abbreviation for the **C**entral **F**armers Fertilizer Company.

Figure 6-23 and Figure 6-24 (below) show the median and mode, respectively, of the break-even ammonia prices for onshore, offshore wind, and offshore geothermal alternatives. In the plots the rate of subsidies (x-axis) is the proportion of capital expenses covered by some outside entities (for instance, the state):

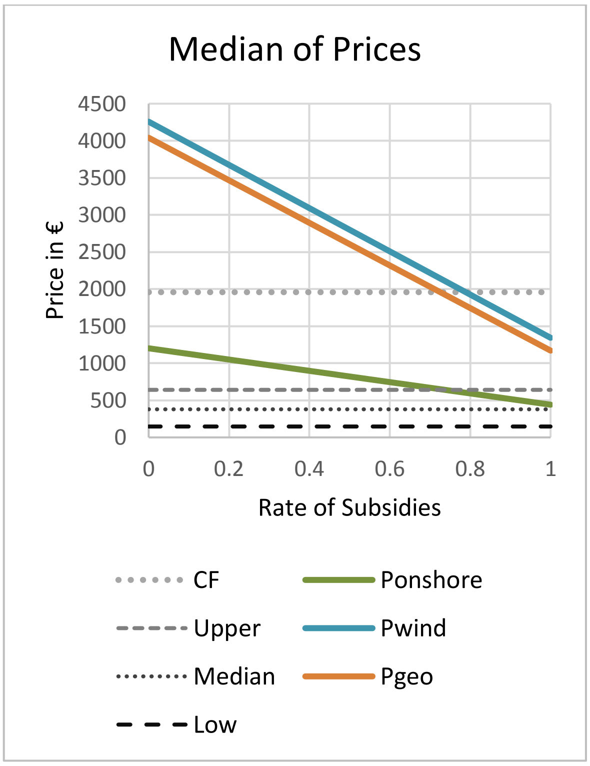

*Figure 6-23: Median of Prices given rate of subsidies (proportion of capital expense covered by outside entities). **CF** is the CF Industries estimate. **Upper**, **Median** and **Low** are the respective estimates of Nayak-Luke and Bañares-Alcántara (2020)*

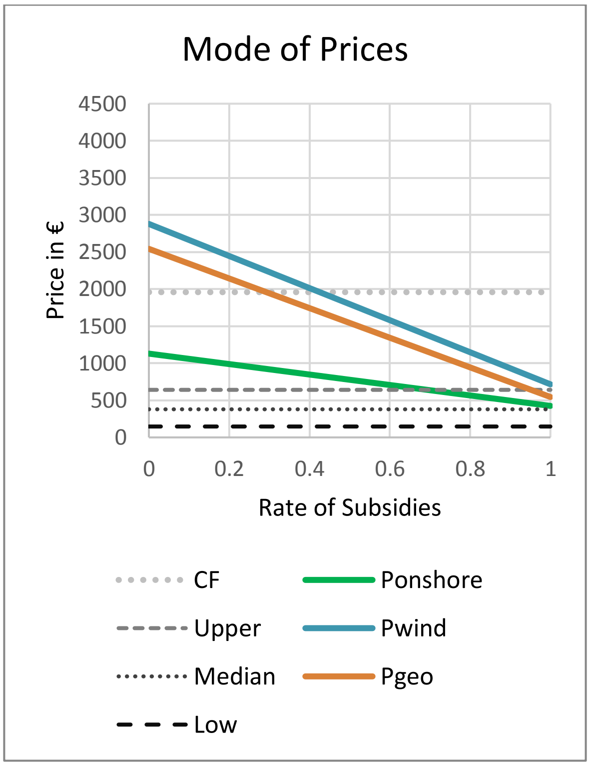

*Figure 6-24: Mode of Prices given rate of subsidies (proportion of capital expense covered by outside entities). **CF** is the CF Industries estimate. **Upper**, **Median** and **Low** are the respective estimates of Nayak-Luke and Bañares-Alcántara (2020)*

Out of our price estimates the ones for $P_{onshore}$ are likely to be the most reliable and in line with actual projects in the real world. The reason there is greater uncertainty about P_{wind} and P_{geo}, as well as the potential of extreme values for both.

Our results indicate the need for subsidies to incentivize offshore (and maybe even onshore) green ammonia production. However, this would not be a perfect remedy for the offshore alternatives, as shown by the following figure:

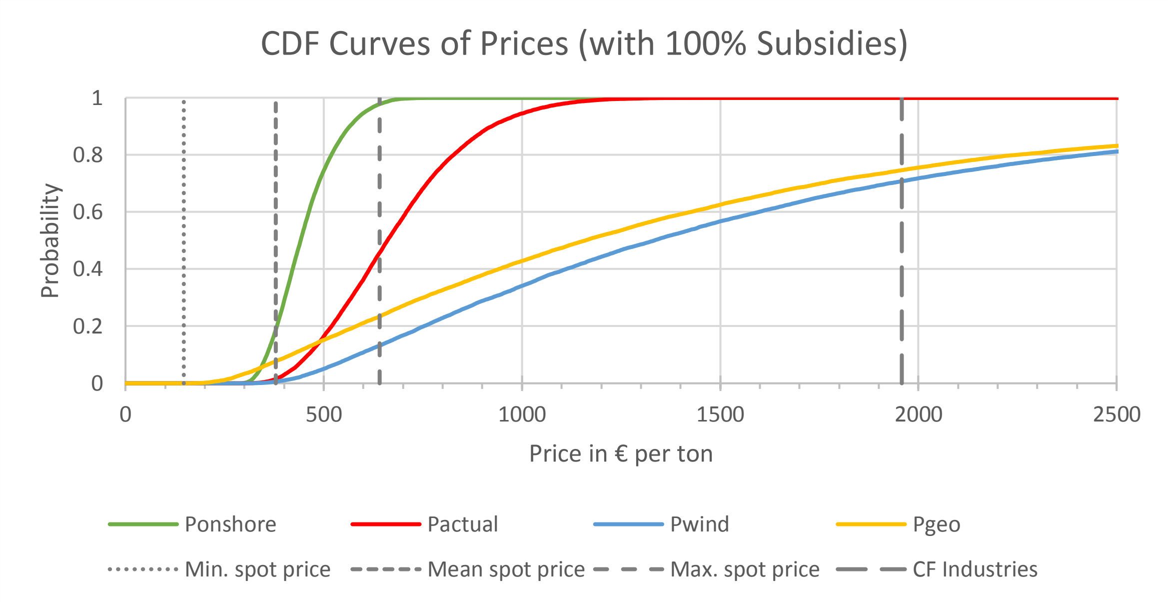

Figure 6-25: CDF Curves of Prices, assuming 100% subsidies. ***CF Industries*** *is the CF Industries estimate.* ***Upper***, ***Median*** *and* ***Low*** *are the respective estimates of Nayak-Luke and Bañares-Alcántara (2020)*

Even with 100% subsidies outliers could still bring the break-even price of P_{wind} and P_{geo} above the highest price estimates.

6.9. Implications for the Profitability of Offshore Green Ammonia (OGA)

6.9.1. Price of Ammonia

The profitability of green ammonia depends on a variety of factors, not least its market price. This price is affected by a great many factors, which are outside the scope of this thesis. However, there are circumstances in which green ammonia production could, in itself, be profitable. In this thesis we have and continue to assume that these circumstances are met.

Our focus here is on the profitability of offshore green ammonia (OGA), and the likelihood that the market (or actual) price of green ammonia exceed break-even prices. Assuming that our calculations for P_{wind} and P_{geo} are mostly in line with reality, a sufficient level of subsidization would push their median below the highest market estimates we have found in our literature review (see Figure 6-23). While a lower degree of subsidization could push their modes below the highest market prices estimate.

We should also bear in mind that we are assuming a premium, *xPrice* (such that $P_{actual} = P_{onshore} \times xPrice$), for having our green ammonia delivered offshore. While the estimates we found in our literature review were for green ammonia delivered onshore.

Therefore, it seems that OGA could be viable, but it is likely to require fairly high ammonia prices and/or subsidies.

6.9.2. NPV

In section 6.5. we presented a series of graphs indicating how NPV (in binary terms of positive or negative) is affected by the platform capital expense (as x_2) and daily production of ammonia (as x_1). This was marked by lines denoting probabilities of positive NPV, with the probability of positive NPV being strictly increasing as x_2 decreases (see Table 6-6 for x_2). We also showed how these statistical models did when tested against other datasets (see section 6.6. and 6.7. , as well as Table 6-7)

So, if our decision maker has an expert estimate of capital expense for an offshore platform given daily ammonia production, we can easily estimate the probability of a positive NPV using our model.

6.10. Opportunities for Future Work

There are many opportunities for future work, however we these appear the most important and promising.

6.10.1. Determining the Link Between Offshore Platform CapEx and Daily Ammonia Production.

As we mentioned earlier (in section 4.6.2.) there is no general formula for the size of an ammonia plant, that is in terms of volume, weight, and floor area. Also, as mentioned in the same section, there exists no general formula for the capital expense or maintenance and operations costs of an offshore platform. Thus, by extension, there is no formula for the relationship between daily ammonia production of a plant, and the capital expense of a platform capable of physically carrying said plant.

Initially we tried to solve the problem by the following approach for estimating the platform capital expense. Using google maps we found satellite pictures of onshore ammonia production facilities, and compared their sizes to the known floor areas of offshore oil platforms. This involves a very limited sample size, as well as the fact that a platform might stack facilities higher and have ammonia storage tanks in its legs or in containers under the sea. We were not able to create a satisfactory solution, but the approach may have merit.

Progress in this area (regardless of approach) would immensely reduce the uncertainties that we are currently dealing with. Although a general equation would be ideal, any sort of algorithm, even with large error bars, would be a great improvement over simply testing the various possible values in a Monte Carlo simulation.

6.10.2. Examining the Effect of Mixing Solar and Wind Power.

In this thesis we have assumed that we will only be using wind power, this greatly simplified our scheme, but also meant that our overall system would be less efficient. We could benefit from studying the effect of blending some proportion of solar and wind power.

6.10.3. Investigating Different Approaches to Ammonia Production

One of the problems with ammonia production is that the ammonia synthesis is not amenable to intermittent operation. It does however require far less energy than the hydrogen electrolysis. Further hydrogen electrolysis can be held in hot standby (whereby it requires far less energy than in the production phase) and quickly ramped up to production. Some new hydrogen electrolysis systems (PEM) are even capable of going from cold standby to production in seconds.(Rouwenhorst, Krzydwa, et al., 2020)

An implication of this is that if there is a variable energy supply, such as a mix of wind and solar power, you can produce excess hydrogen when the energy supply is high. Store the hydrogen, and then, when energy supply decreases, you ramp down hydrogen production and use the stored hydrogen to keep the ammonia synthesis running.(Nayak-Luke & Bañares-Alcántara, 2020)

The general conclusion from this is that we would not require as much energy storage, nor excess wind power capacity, to deal with variations in wind strength. This would reduce both capital expenses and operating expenses.

6.10.4. Further Investigation Into Offshore Geothermal Energy

Other than Karason (2013) we were unable to find any studies on the cost of offshore geothermal power. It is however a very interesting technology, offering large amounts of reliable energy. Further, geothermal is most accessible offshore in various ridges and subduction zones (Banerjee et al., 2018) that just so happens to cross or be very near to major shipping lanes in the Pacific and Atlantic.

Since we have elsewhere held up the possibility of a premium for supplying green ammonia at sea (*xPrice*), geothermal energy seems obviously interesting.

6.10.5. Investigation Into the Likelihood of Receiving Subsidies and Their Magnitudes

White et al. (2013) point out that the consistency of government support is also of vital importance for investor confidence. As we mentioned before (sections 4.3.), the magnitude and likelihood of potential subsidies has a great impact on whether a project will be economically viable

So, governmental support and subsidies are key factors for any investment decisions. Since there is great uncertainty on the topic, reducing this uncertainty is highly relevant and material to any decisions on investing in green ammonia.

7. Conclusion

The goal of this thesis is to provide useful insight to support the decision on whether an energy company should invest in an offshore green ammonia (OGA) plant. Towards this aim, we have developed a decision analysis framework for OGA production. Within this framework we have: we have used an influence diagram to give context to the decision problem; identified key, relevant uncertainties and their ranges through a literature review; formulated economic models for OGA production; performed sensitivity analysis to identify material uncertainties; and performed Monte Carlo simulation to assess the economic, in term of net present value (NPV), uncertainty of OGA production. Such a decision analysis approach has effectively transformed the decision problem from being opaque to transparent (i.e., clearly understood and communicated).

Based on the Monte Carlo simulation results, we have built the statistical models for assessing predict the probability of a positive NPV (i.e., an OGA plant is profitable) if a decision maker provides a daily ammonia production capacity and a capital expense of the offshore platform (adjusted for any subsidies).

We have further narrowed the number of statistical models from six down to two: one for offshore wind power and another for offshore geothermal power (section 6.7. and appendix A).

From the statistical models, we have generated a graph of the probability lines for each of the models. See appendix B for a large scale version of these graphs, or see section 6.4.1. for an explanation of how the graphs work. These graphs allow for quick probability estimates by seeing where daily production (x_1) and modified capital expense (x_2) cross, and also provides an overall indication of how likely the project is to have a positive NPV.

In our suggestions for future research (section 6.10.) we have brought up a variety of subjects that are most relevant and material to offshore green ammonia investment decisions, such as: the relationship between production capacity (in tons of ammonia per day) and the cost of the necessary offshore platform; effects of using both wind and solar power; different production techniques (constant hydrogen productions vs stockpiling for later use); the future of offshore geothermal power; and the likelihood, scale and dependability of government subsidies.

In conclusion since green ammonia production is energy demanding, shifting it out to ses would free up onshore and near-shore energy for other onshore uses. So OGA is a potentially promising solution to the conflicts that surround the use of coastal waters (see section 3.4. and Tiller et al. (2012) for examples). At the same time offshore energy (that would otherwise not be effectively used) could be turned into a green fuel – ammonia. OGA production appears technically viable, but we are uncertain about its economic viability (whether an OGA project would have a positive NPV). Therefore, we recommend that further studies (such as the ones we recommended) should be carried out.

Bibliography

Alnes, O., Eriksen, S., & Vartdal, B. (2017). Battery-Powered Ships: A Class Society Perspective. *IEEE Electrification Magazine, 5*(3), 10-21. doi:10.1109/MELE.2017.2718823

Armijo, J., & Philibert, C. (2020). Flexible production of green hydrogen and ammonia from variable solar and wind energy: Case study of Chile and Argentina. *International Journal of Hydrogen Energy, 45*(3), 1541-1558.

Aspelund, A., Steen, M., Afewerki, S., Bjørgum, Ø., Sæther, E. A., & Kenzhegaliyeva, A. (2019). Conditions for growth in the Norwegian offshore wind industry. International market developments, Norwegian firm characteristics and strategies, and policies for industry development.

Austgulen, M. H. (2012). *Nordmenns holdninger til klimaendringer, medier og politikk*. Oslo: Statens institutt for forbruksforskning.

Banerjee, A., Chakraborty, T., & Matsagar, V. (2018). Evaluation of possibilities in geothermal energy extraction from oceanic crust using offshore wind turbine monopiles. *Renewable and Sustainable Energy Reviews, 92*, 685-700. Retrieved from https://www.sciencedirect.com/science/article/pii/S1364032118303319. doi:https://doi.org/10.1016/j.rser.2018.04.114

Bratvold, R. B., & Begg, S. (2010). *Making good decisions* (Vol. 207): Society of Petroleum Engineers Richardson, Texas.

Brier, G. W. (1950). Verification of forecasts expressed in terms of probability. *Monthly weather review, 78*(1), 1-3.

Brown, T. (2018). *Innovations in Ammonia*. Paper presented at the H2@Scale R&D Consortium Kick-Off Meeting, Chicago. https://www.energy.gov/sites/prod/files/2018/08/f54/fcto-h2-scale-kickoff-2018-10-burgunder.pdf

Brown, T. (2020). Viking Energy to be retrofit for ammonia fuel in 2024. Retrieved from https://www.ammoniaenergy.org/articles/viking-energy-to-be-retrofit-for-ammonia-fuel-in-2024/

Bull, M. (1968). *Development of an ammonia-burning gas turbine engine*. Retrieved from

De Vries, N., Okafor, E., Gutesa-Bozo, M., Xiao, H., & Valera-Medina, A. (2020). Use of Ammonia for Heat, Power and Propulsion. In *Techno-Economic Challenges of Green Ammonia as an Energy Vector* (pp. 105-154): Academic Press.

Demirhan, C. D., Tso, W. W., Powell, J. B., & Pistikopoulos, E. N. (2019). Sustainable ammonia production through process synthesis and global optimization. *AIChE Journal, 65*(7), e16498.

Dietz, S., Bowen, A., Doda, B., Gambhir, A., & Warren, R. (2018). The Economics of 1.5°C Climate Change. *Annual Review of Environment and Resources, 43*(1), 455-480. Retrieved from https://www.annualreviews.org/doi/abs/10.1146/annurev-environ-102017-025817. doi:10.1146/annurev-environ-102017-025817

Djinović, P., & Schüth, F. (2015). Energy carriers made from hydrogen. In *Electrochemical Energy Storage for Renewable Sources and Grid Balancing* (pp. 183-199): Elsevier.

Dobson, A. J., & Barnett, A. G. (2018). *An introduction to generalized linear models*: CRC press.

Fawcett, T. (2006). An introduction to ROC analysis. *Pattern recognition letters, 27*(8), 861-874.

Gardiner, P. D. (2005). *Project management: A strategic planning approach*: Macmillan International Higher Education.

Halvorsen, K. (2009). *Spørsmål nr. 672 til skriftlig besvarelse fra Trine Skei Grande om økt tilrettelegging for bruk av elbil* Regjeringen Stoltenberg II: Finansdepartementet

Hillier, D., Ross, S., Westerfield, R., Jaffe, J., & Jordan, B. (2018). *Corporate finance* (5th ed.): McGraw Hill.

Holttinen, H. (2005). Hourly wind power variations in the Nordic countries. *Wind Energy: An International Journal for Progress and Applications in Wind Power Conversion Technology, 8*(2), 173-195.

Kailos, N. C. (1966). *Utilization of ammonia as an alternate fuel in army aircraft engines* (Vol. 66): US Army Aviation Materiel Laboratories.

Karason, B. (2013). *Utilization of offshore geothermal resources for power production.*

Kikuchi, Y., & Ishihara, T. (2019). *Upscaling and levelized cost of energy for offshore wind turbines supported by semi-submersible floating platforms* Paper presented at the EERA DeepWind'19, Trondheim. https://www.sintef.no/globalassets/project/eera-deepwind-2019/presentations/e2_yukakikuchi20190117r.pdf

Kyoto Protocol. (1997). UNFCCC

Laursen, R. (2018). *Ship operation using LPG and ammonia as fuel on MAN B&W dual fuel ME-LGIP engines.* Paper presented at the Proceedings of the NH3 Fuel Conference.

Lim, D.-K., Plymill, A. B., Paik, H., Qian, X., Zecevic, S., Chisholm, C. R. I., & Haile, S. M. (2020). Solid Acid Electrochemical Cell for the Production of Hydrogen from Ammonia. *Joule, 4*(11), 2338-2347. Retrieved from https://www.sciencedirect.com/science/article/pii/S2542435120304955. doi:https://doi.org/10.1016/j.joule.2020.10.006

Lund, P., & Paatero, J. (2006). Energy storage options for improving wind power quality. *imu*, 2002.

Morgan, E. R., Manwell, J., & McGowan, J. (2014). Wind-powered ammonia fuel production for remote islands: A case study. *Renewable Energy, 72*, 51-61.

Morgan, E. R., Manwell, J. F., & McGowan, J. G. (2017). Sustainable ammonia production from US offshore wind farms: a techno-economic review. *ACS Sustainable Chemistry & Engineering, 5*(11), 9554-9567.

Nayak-Luke, R. M., & Bañares-Alcántara, R. (2020). Techno-economic viability of islanded green ammonia as a carbon-free energy vector and as a substitute for conventional production. *Energy & Environmental Science, 13*(9), 2957-2966.

Nayak-Luke, R. M., Forbes, C., Cesaro, Z., Bañares-Alcántara, R., & Rouwenhorst, K. H. R. (2020). Storage and Distribution of Ammonia. In *Techno-Economic Challenges of Green Ammonia as an Energy Vector* (pp. 191-207): Academic Press.

Norwegian Ministry of Petroleum and Energy and Norwegian Ministry of Climate and Environment. (2020). *The Norwegian Government's hydrogen strategy* (Y-0127 E). Norwegian Ministry of Petroleum and Energy and Norwegian Ministry of Climate and Environment Retrieved from https://www.regjeringen.no/contentassets/40026db2148e41eda8e3792d259efb6b/y-0127e.pdf

NRK. (2021). Elektriske ferjer. *NRK*. Retrieved from https://www.nrk.no/nyheter/elektriske-ferjer-1.14323794

Paris Agreement. (2016). UNFCCC

Pearson, R. J., Eisaman, M. D., Turner, J. W., Edwards, P. P., Jiang, Z., Kuznetsov, V. L., . . . Taylor, S. G. (2011). Energy Storage via Carbon-Neutral Fuels Made From CO_2, Water, and Renewable Energy. *Proceedings of the IEEE, 100*(2), 440-460.

Pidgeon, N., Poortinga, W., Steentjes, K., Corner, A., Mays, C., Poumadère, M., . . . University of Wales, C. (2017). *European Perceptions of Climate Change (EPCC) :*

topline findings of a survey conducted in four European countries in 2016: [Cardiff University].

Rouwenhorst, K. H. R., Elishav, O., Lis, B. M., Grader, G., Mounaïm-Rousselle, C., Roldan, A., & Valera-Medina, A. (2020). Future Trends. In *Techno-Economic Challenges of Green Ammonia as an Energy Vector* (pp. 303-319): Academic Press.

Rouwenhorst, K. H. R., Krzydwa, P. M., Benes, N. E., Mul, G., & Lefferts, L. (2020). Ammonia Production Techniques. In *Techno-Economic Challenges of Green Ammonia as an Energy Vector* (pp. 41-84): Academic Press.

Royal Society. (2020). Ammonia: Zero-Carbon Fertiliser, Fuel and Energy Store. In: The Royal Society London, UK.

Samferdselsdepartementet. (2020). *CO2-utslippskrav til person- og varebiler (revisjon)*. EØS-notatbasen: Parlament og Råd

Sánchez, A., & Martín, M. (2018a). Optimal renewable production of ammonia from water and air. *Journal of Cleaner Production, 178*, 325-342. Retrieved from https://www.sciencedirect.com/science/article/pii/S0959652617332730. doi:https://doi.org/10.1016/j.jclepro.2017.12.279

Sánchez, A., & Martín, M. (2018b). Scale up and scale down issues of renewable ammonia plants: Towards modular design. *Sustainable Production and Consumption, 16*, 176-192. Retrieved from https://www.sciencedirect.com/science/article/pii/S2352550918300812. doi:https://doi.org/10.1016/j.spc.2018.08.001

Saul, J., & Chestney, N. (2020). First wave of ships explore green hydrogen as route to net zero. *Reuters*. Retrieved from https://www.reuters.com/article/shipping-energy-hydrogen-focus-int-idUSKBN27F18U

Seaman, R. W., & Huson, G. (2011). *The choice of NH3 to fuel the X-15 rocket plane.* Paper presented at the 8th NH3 Fuel Association Conference.

Statens Vegvesen. (2020). *«En stille revolusjon i norske fjorder»*. Retrieved from https://www.vegvesen.no/_attachment/2796219/binary/1341772?fast_title=En+stille+revolusjon+i+norske+fjorder.+Innovasjon+-+utviklingskontrakt.pdf

Stern, N. H., Peters, S., Bakhshi, V., Bowen, A., Cameron, C., Catovsky, S., . . . Edmonson, N. (2006). *Stern Review: The economics of climate change* (Vol. 30): Cambridge University Press Cambridge.

Stuart, A. A. (1929, September). A Nine-Acre Nest for Dirigibles. *Popular Science*, 20-21.

The United Nations Framework Convention on Climate Change (UNFCCC). (1992).

Thomas, C. (2009). Fuel cell and battery electric vehicles compared. *International Journal of Hydrogen Energy, 34*(15), 6005-6020.

Tiller, R., Brekken, T., & Bailey, J. (2012). Norwegian aquaculture expansion and Integrated Coastal Zone Management (ICZM): Simmering conflicts and competing claims. *Marine Policy, 36*(5), 1086-1095. doi:10.1016/j.marpol.2012.02.023

Timperley, J. (2020). The fuel that could transform shipping. *BBC*. Retrieved from https://www.bbc.com/future/article/20201127-how-hydrogen-fuel-could-decarbonise-shipping

Tollaksen, T. G. (2021). Han vil bygge verdens første drivstoffstasjon ute i havet. *E24*. Retrieved from https://e24.no/det-groenne-skiftet/i/QmjLK4/han-vil-bygge-verdens-foerste-drivstoffstasjon-ute-i-havet?utm_source=email

Toralde, J. S. S. (2014). *Offshore Geothermal Energy Utilisation: An Idea Whose Time Has Come?* Paper presented at the Offshore Technology Conference-Asia.

Tullo, A. H. (2021, March 8). Is ammonia the fuel of the future? . *Chemical & Engineering News*. Retrieved from https://cen.acs.org/business/petrochemicals/ammonia-fuel-future/99/i8

Valera-Medina, A., & Banares-Alcantara, R. (2020a). Introduction. In *Techno-Economic Challenges of Green Ammonia as an Energy Vector* (pp. 1-14): Academic Press.

Valera-Medina, A., & Banares-Alcantara, R. (Eds.). (2020b). *Techno-Economic Challenges of Green Ammonia as an Energy Vector*: Academic Press.

Van Duyne, S. (1941, August). From Cook Stoves to Tanks ... They Roll from the Automobile Factories. *Popular Science*, 114-121.

van Renssen, S. (2020). The hydrogen solution? *Nature Climate Change, 10*(9), 799-801.

White, W., Lunnan, A., Nybakk, E., & Kulisic, B. (2013). The role of governments in renewable energy: The importance of policy consistency. *Biomass and bioenergy, 57*, 97-105.

Wiser, R., Jenni, K., Seel, J., Baker, E., Hand, M., Lantz, E., & Smith, A. (2016). Expert elicitation survey on future wind energy costs. *Nature Energy*, *1*(10), 1-8.

Ytterstad, A. (2011). Klimakrisen utfordrer objektivitetsidealet i norsk journalistikk. *Norsk medietidsskrift*(04), 323-343.

Appendix

A. Our Best Statistical Models for Wind and Geothermal Power

We have in section 6.7. shown that the NS models are superior in terms of PPV, and equally good measured by the Brier Score. In this section of the appendix we merely seek to present relevant figures, equations, programming samples, and so on for the readers convenience.

A.1. Parameters and Equations

Let us first quickly define our key variables:

$$x_1 = TonsPrDay \quad \text{(A-1)}$$

$$x_2 = CapExPlatform(1 - SubProp) \quad \text{(A-2)}$$

To our right we have Table A-1 of the parameters of the winning NS statistical model (for calculating the probability of a positive NPV).

The accompanying equations are presented below.

$$P(NPVpos|\boldsymbol{X}) = \frac{1}{1 + \exp(-\boldsymbol{x}'\boldsymbol{\beta})} \quad \text{(A-3)}$$

$$\begin{aligned} \boldsymbol{x}'\boldsymbol{\beta} = \beta_0 + \beta_{11}x_1 + \beta_{12}x_1^2 \\ + \beta_{13}x_1^3 + \beta_{21}x_2 \\ + \beta_{22}x_2^2 + \beta_{23}x_2^3 \\ + \beta_{24}x_2^4 + \beta_{25}x_2^5 \\ + \beta_{26}x_2^6 \end{aligned} \quad \text{(A-4)}$$

NS MODEL		
	Offshore Wind Power	Geothermal Power
β_0	2.075e-01	4.448e-01
β_{11}	7.172e-03	8.609e-03
β_{12}	-3.210e-06	-3.993e-06
β_{13}	6.514e-10	8.108e-10
β_{21}	-4.123e-03	-3.803e-03
β_{22}	1.226e-06	8.863e-07
β_{23}	-2.143e-10	-1.235e-10
β_{24}	1.929e-14	9.189e-15
β_{25}	-8.429e-19	-3.415e-19
β_{26}	1.379e-23	4.918e-24

Table A-1: Parameters for the NS model

That is equation (A-3) is the probability of a positive NPV given a set of given values for x_1 and x_2.

This model holds for $x_1 \in [250\,, 2000]$ and $x_2 \in [0\,, 22000]$ proof of the latter can be found in appendix C.

A.2. Python Code

Since Table A-1 may be somewhat confusing or hard to type in, we are including this Python code suitable for cutting and pasting.

```
# BEGIN CODE

import math

# Wind power for the No Subsidies model

def FuncPxWindNS(TonsPerDay, CapEx):

    b0 = 2.075e-01

    b11 = 7.172e-03

    b12 = -3.210e-06

    b13 = 6.514e-10

    b21 = -4.123e-03

    b22 = 1.226e-06

    b23 = -2.143e-10

    b24 = 1.929e-14

    b25 = -8.429e-19

    b26 = 1.379e-23


    x1 = float(TonsPerDay)

    x2 = float(CapEx)

    Px = 1/(1+math.exp(-(b0+b11*x1+b12*x1**2+b13*x1**3+

            b21*x2+b22*x2**2+b23*x2**3+b24*x2**4+b25*x2**5+b26*x2**6)))

    return Px

# Geothermal for the No Subsidies model

def FuncPxGeoNoSub(TonsPerDay, CapEx):
```

```
    b0 = 4.448e-01
    b11 = 8.609e-03
    b12 = -3.993e-06
    b13 = 8.108e-10
    b21 = -3.803e-03
    b22 = 8.863e-07
    b23 = -1.235e-10
    b24 = 9.189e-15
    b25 = -3.415e-19
    b26 = 4.918e-24
    x1 = float(TonsPerDay)
    x2 = float(CapEx)
    Px = 1/(1+math.exp(-(b0+b11*x1+b12*x1**2+b13*x1**3+
            b21*x2+b22*x2**2+b23*x2**3+b24*x2**4+b25*x2**5+b26*x2**6)))
    return Px
# END CODE
```

A.3. Excel Code

If you are more comfortable working with Excel it should be possible to copy and paste this into an excel spreadsheet:

	A	B	C	D	E	F
1	Parameter	Wind	Geo		TonsPrDay	CapEx
2	b0	2.08E-01	4.45E-01		250	0
3	b11	7.17E-03	8.61E-03		P(Wind)	P(Geo)
4	b12	-3.21E-06	-3.99E-06		F1	F2
5	b13	6.51E-10	8.11E-10			
6	b21	-4.12E-03	-3.80E-03			
7	b22	1.23E-06	8.86E-07			
8	b23	-2.14E-10	-1.24E-10			
9	b24	1.93E-14	9.19E-15			
10	b25	-8.43E-19	-3.42E-19			
11	b26	1.38E-23	4.92E-24			

But for F1 insert:

```
=1/(1+EXP(-(B2+B3*$E$2+B4*$E$2^2+B5*$E$2^3+B6*$F$2+B7*$F$2^2+B8*$F$2^3+B9*$F$2^4+B10*$F$2^5+B11*$F$2^6)))
```

And for F2 insert:

```
=1/(1+EXP(-(C2+C3*$E$2+C4*$E$2^2+C5*$E$2^3+C6*$F$2+C7*$F$2^2+C8*$F$2^3+C9*$F$2^4+C10*$F$2^5+C11*$F$2^6)))
```

B. Probability Graphs of NPVPos

As we mentioned in sections 6.4. and 6.4.1. since we can calculate the probability for $P(NPVpos|\boldsymbol{X})$ for any given value of $\boldsymbol{X} = [x_1, x_2]$, and we know that our statistical models are strictly decreasing, then we can always calculate $x_2(p, x_1)$. That is for any given: $p = n_1, x_1 = n_2$ where $p \in [0.05,1)$ and $x_1 \in [250\ ,2000]$, there is a unique corresponding x_2.

Thus, it is possible to draw a probability line of any $p \in [0.05,1)$ so long as $x_1 \in [250\ ,2000]$ and $x_2 \in [0\ ,22000]$, and the two axis of the graph are x_1 and x_2.

In previous sections it would take up too much space to have a full-sized graph. However, such graphs might be a good decision aid, and so they are included here. Please note that the Wind Power graph has CapEx go from 0 to 9000 million €, while the Geothermal Power graph has CapEx go from 0 to 12 000 million €.

B.1. Probability Line Graph for Offshore Wind Power

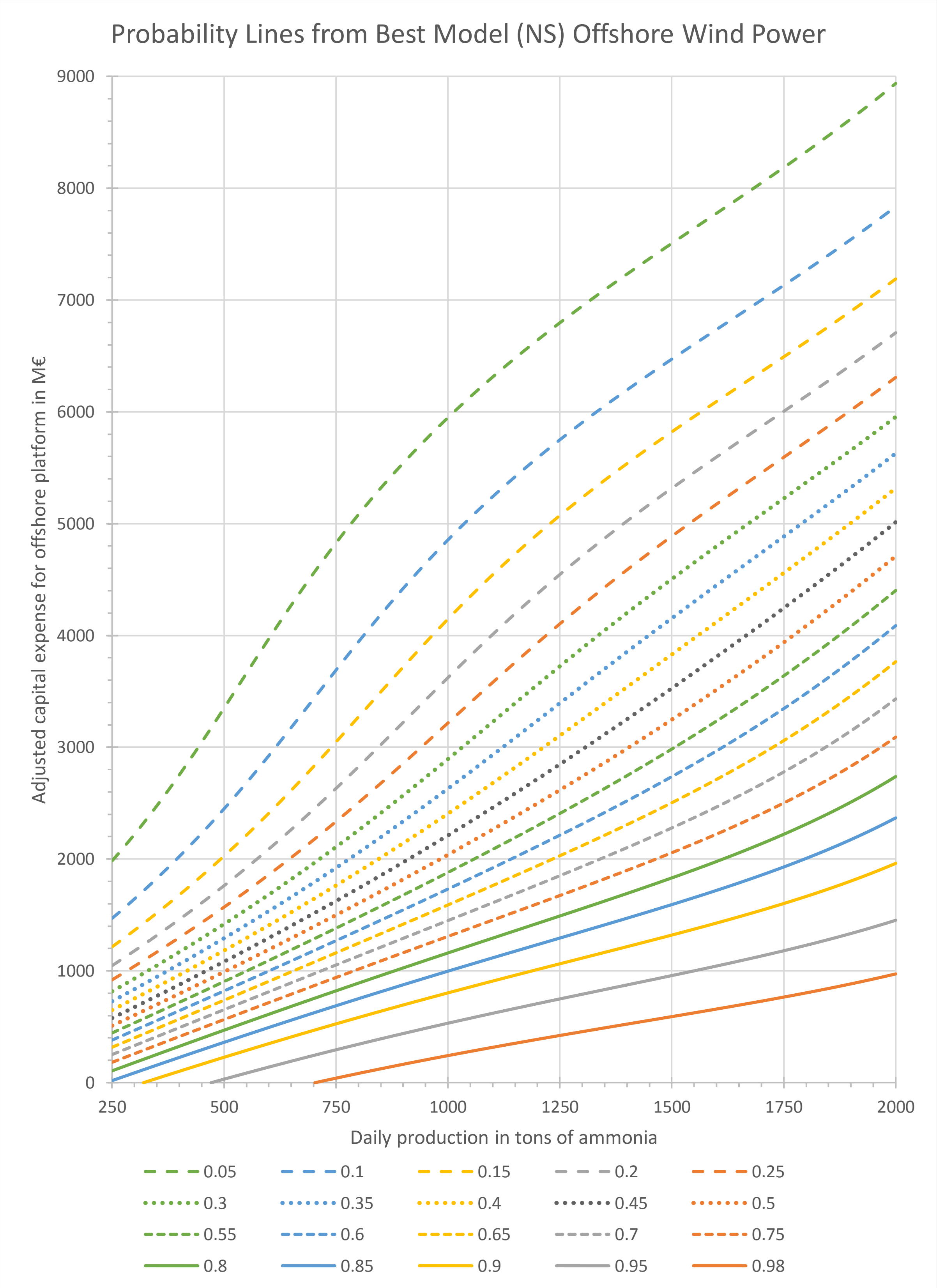

Figure B-1: Probability Lines from Best Model (NS) Offshore Wind Power

B.2. Probability Line Graph for Offshore Geothermal Power

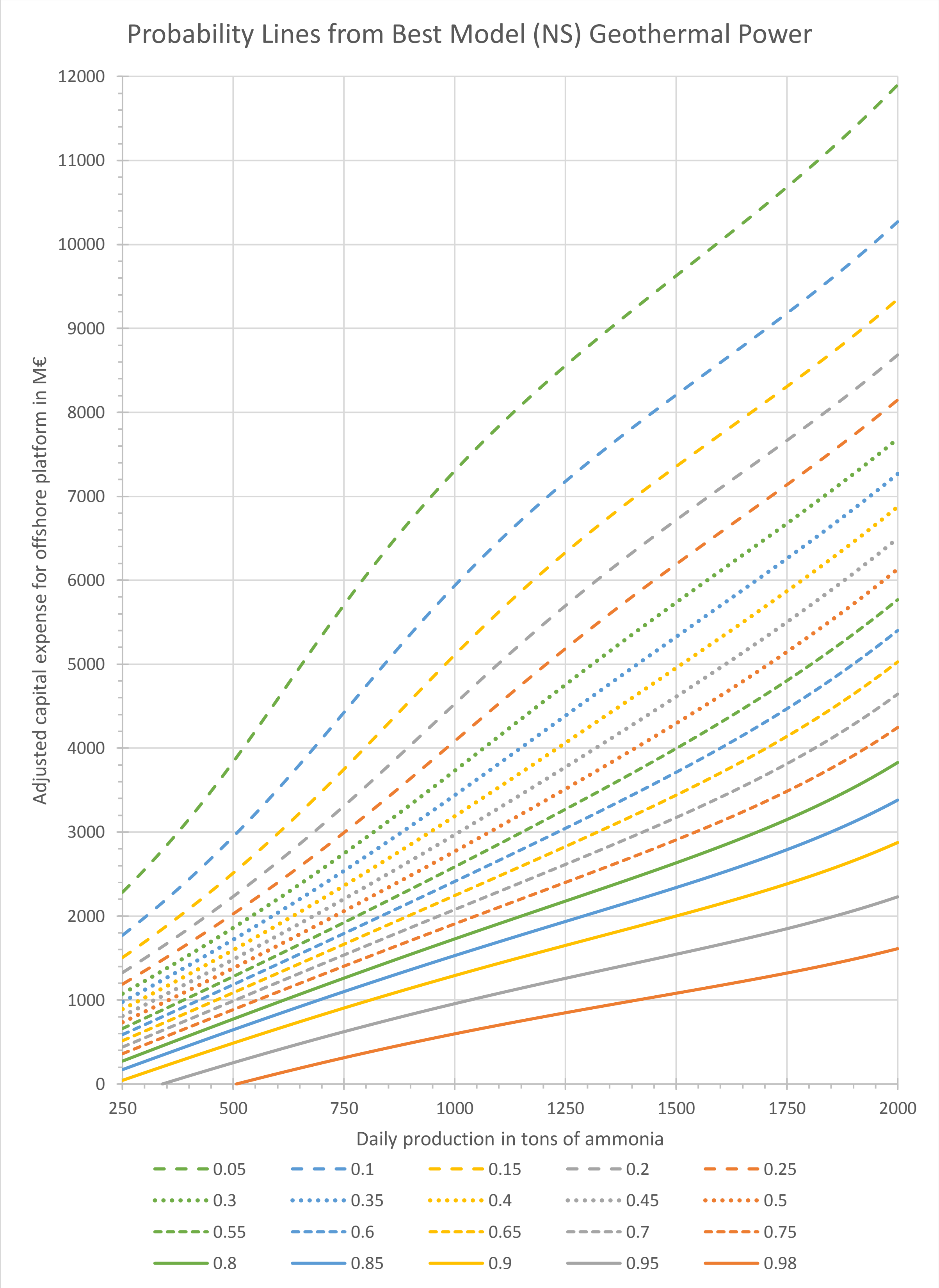

Figure B-2:Probability Lines from Best Model (NS) Offshore Geothermal Power

C. Proof That Probabilities in Our Statistical Models are Strictly Decreasing

To be precise what we want to prove is that for any value of TonsPrDay (x_1) our probability $P(NPVpos|\boldsymbol{X})$ where $\boldsymbol{X} = [x_1, x_2]$ will be strictly decreasing as the capital expense of the offshore platform (x_2) is increasing.

So, with:

$$\begin{aligned} x_1 &= \text{Tons per day} \\ x_2 &= \text{CapExPlatform in millions of €} \end{aligned} \tag{C-1}$$

We have that:

$$P(NPVpos|\boldsymbol{X}) \ = \frac{1}{1 + \exp(-\boldsymbol{x}'\boldsymbol{\beta})} \tag{C-2}$$

$$\begin{aligned} \boldsymbol{x}'\boldsymbol{\beta} = \beta_0 + \beta_{11}x_1 + \beta_{12}x_1^2 + \beta_{13}x_1^3 + \beta_{14}x_1^4 + \beta_{21}x_2 + \beta_{22}x_2^2 \\ + \beta_{23}x_2^3 + \beta_{24}x_2^4 + \beta_{25}x_2^5 + \beta_{26}x_2^6 \end{aligned} \tag{C-3}$$

But, since we have some given x_1 this can be reduced to:

$$f(x_2) \ = \frac{1}{1 + \exp(-p(x_2))} \tag{C-4}$$

$$p(x_2) = \beta_{0'} + \beta_{21}x_2 + \beta_{22}x_2^2 + \beta_{23}x_2^3 + \beta_{24}x_2^4 + \beta_{25}x_2^5 + \beta_{26}x_2^6 \tag{C-5}$$

We can now decide where *f* is strictly decreasing by differentiating, and then seeing where the derivative is less than zero.

$$\frac{d}{dx_2}f(x_2) \ = \frac{p'(x_2)}{\exp(p(x_2)) \times \left(1 + \exp\left(-p(x_2)\right)\right)} \tag{C-6}$$

$$p'(x_2) = \beta_{21} + 2\beta_{22}x_2 + 3\beta_{23}x_2^2 + 4\beta_{24}x_2^3 + 5\beta_{25}x_2^4 + 6\beta_{26}x_2^5 \tag{C-7}$$

Since the denominator is necessarily positive we need only plot where $p'(x_2) < 0$ to see where our probability $P(NPVpos|\boldsymbol{X})$ is strictly decreasing.

If we look at the graphs below we see that all of our statistical models are strictly decreasing for $x_2 \in [0\ , 22000]$.

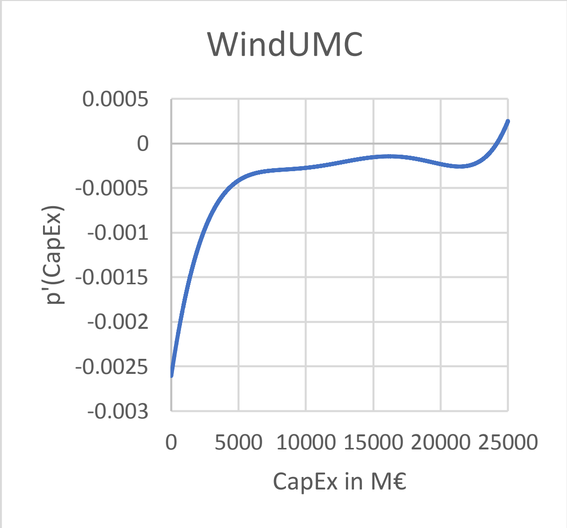

Figure C-1: Graph of p'(CapEx) for WindUMC model

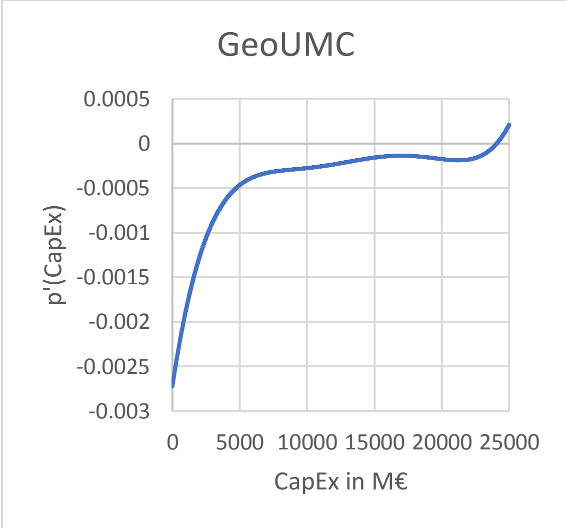

Figure C-2: Graph of p'(CapEx) for GeoUMC model

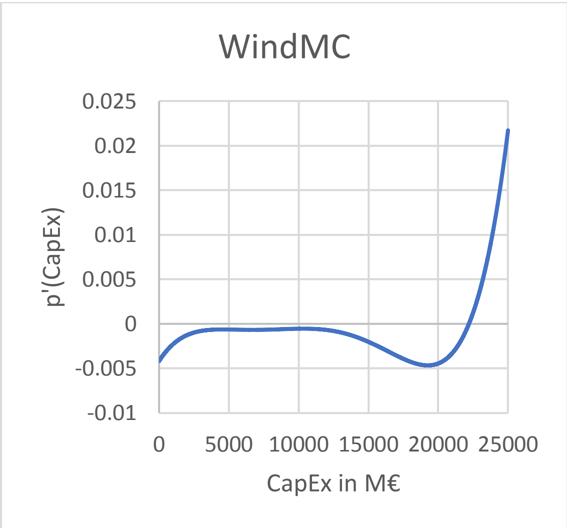

Figure C-3: Graph of p'(CapEx) for WindMC model

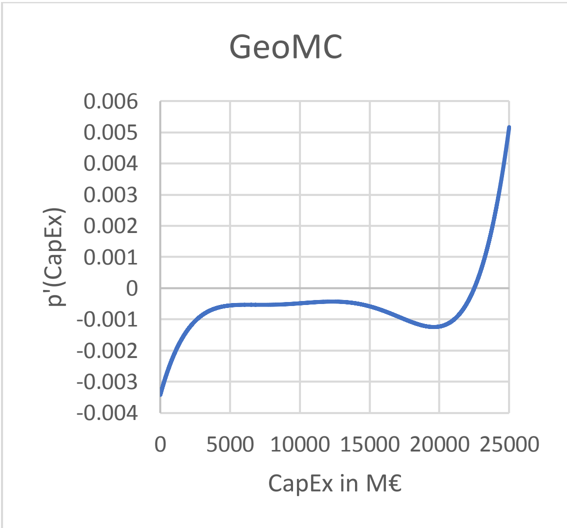

Figure C-4: Graph of p'(CapEx) for GeoMC model

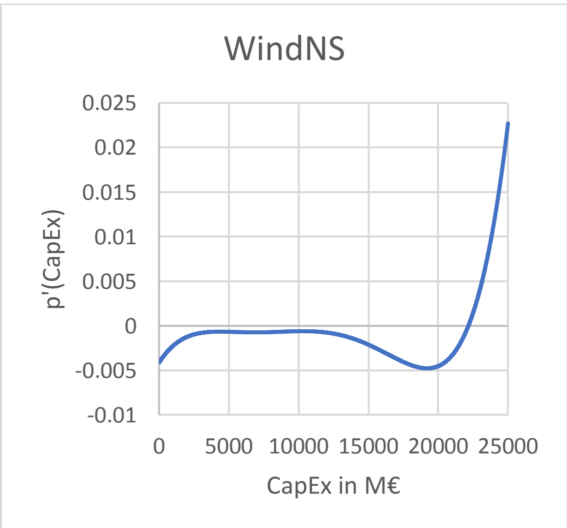

Figure C-5: Graph of p'(CapEx) for WindNS model

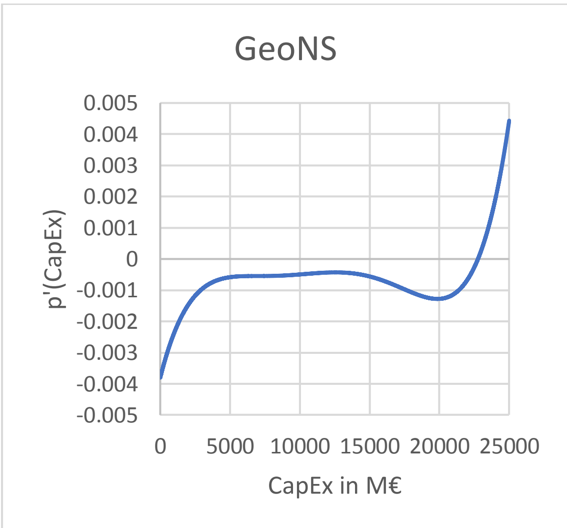

Figure C-6: Graph of p'(CapEx) for GeoNS model